

People's Democratic Republic of Algeria
Ministry of Higher Education and Scientific Research
University M'Hamed BOUGARA – Boumerdès



Institute of Electrical and Electronic Engineering
Department of Control and Power Engineering

Project Report Presented in Partial Fulfilment of
the Requirements of the Degree of

‘MASTER’

In Power Engineering

Title:

**Analysis and design of an analytical MPPT
applied for different converter configurations**

Presented By:

- **DJOUIDER Abderrazak Ziane**
- **TAHIR Mustapha**

Supervisor:

Pr. AISSA KHELDOUN

Co-Spervisor: **Dr. HAMZA BELMADANI.**

2021/2022

Dedication

Dedication

*I have a great pleasure to dedicate
this work To my Beloved Mother, my*

Dear Father Ahmed

To my Dear Sisters :Meriem ,Chayma and Insaf

To all my Friends

Specially Mustapha , Merzoug , Adel and Islem

*To all my Teachers from primary school to my
last year ofuniversity*

And to all with whom I spent wonderful moments

Djouider Abderrazak Ziane

Dedication

Dedication

*I have a great pleasure to dedicate
this work To my Beloved Mother, my*

Dear Father

To my Dear Brother ,Sisters and

To all my Friends

Specially Ziane , Adel,Abdelkoudous and Islem

*To all my Teachers from primary school to my
last year ofuniversity*

And to all with whom I spent wonderful moments

TAHIR MUSTAPHA

Acknowledgement

Acknowledgement

We would like to express our deepest gratitude to our supervisor Pr.AISSA KHELDOUN, for all of his constant support, motivation and friendship throughout the completion of this report. His wide knowledge, logical thinking and wise guidance made it an absolute privilege to work with him.

Special thanks to everyone who had an impact on this work

Absratct

Abstract

This project is intended to analyze the maximum power point tracking constraint conditions of the 12 PV systems under ideal conditions; The constraint conditions are necessary and sufficient conditions to guarantee the existence of the maximum power points of these PV systems. These constraint conditions are expressed by the modal parameters of the PV, therefore they show the inherent relationship between the load and the cell parameters when the maximum power point of the system always exist. In addition to apply them in practice, the maximum power point tracking constraint condition of the practical application are investigated. Furthermore, our work includes the variable weather parameter maximum power point tracking method based on equation solution (ES-VWP method). This equation consists of two analytic equations which represent two different operating points of the PV system. The simulation of this technique has shown a good effectiveness in terms of maximum power point and time response.

Table of contents

Dedications	I
Acknowledgement	III
Abstract	IV
List of figures.....	VIII
List of tables... ..	XI
General introduction	1

CHAPTER 1

PV modelling

1.1 Introduction	4
1.2 Solar photovoltaic system	4
1.2.1. Structure of a photovoltaic cell	5
1.3 Equivalent circuit of a solar cell.....	6
1.3.1. Ideal model.....	6
1.3.2. One-diode model taking account only R_s (4-p model)	7
1.3.3. One-diode model considering R_s and R_p (5-p model).....	7
1.3.4. Two-diode model	8
1.4 Open circuit voltage, short circuit current and maximum power point	8
1.5 Temperature and irradiance effect.....	9
1.5.1. Effect of irradiance.....	10
1.5.2. Effect of temperature	11
1.6 Conclusion	12

CHAPTER 2

Converters

2.1 Introduction	14
2.2 DC/DC converters	14
2.2.1 Buck converters.....	14
2.2.2 Boost converters	16
2.2.3 Buck–Boost converter	17
2.3 DC/DC converters for PV application	19
2.4 DC/AC coverter	19
2.4.1 Steps for DC-AC conversion.....	20
2.4.2 Pulse width modulation	21
2.5 Conclusion.....	22

CHAPTER 3

Maximum Power Point Tracking Constraint condition

Table of contents

3.1	Introduction	24
3.2	Integrated modeling of PV system.....	24
3.2.1	PV systems with DDC.....	24
3.2.2	PV systems with DDC and DC bus.....	26
3.2.3	PV system with DDC and inverter.....	26
3.2.4	PV system with DDC, inverter and AC bus.....	27
3.3	MPPTCC under ideal condition	28
3.3.1	Expression of the MPPTCC.....	28
3.3.2	MPPTCC based on four-parameter model of PV cell	32
3.3.3	MPPTCC impractical application	33
3.4	Perturb and observe algorithm	37
3.5	A variable weather parameter MPPT method based on equation solution for photovoltaic system with DC bus	38
3.5.1	The principle of the ES-VWP method.....	38
3.5.1.1	Mathematical modeling of PV system with DC bus.....	38
3.6	Conclusion.....	42

CHAPTER 4

Simulation and discussion

4.1	Introduction.....	44
4.2	Characteristics of C_R and C_c	44
4.3	Accuracy of the MPPTCC.....	45
4.3.1	Test under STC conditions.....	32
4.3.2	Rapidly changing conditions.....	34
4.3.2.1	Change in irradiance.....	34
4.3.2.2	Change in temperature.....	35
4.3.3	Partial shading.....	37
4.4	Feasibility and availability of the proposed method.....	51
4.4.1	Analysis under varying S condition.....	51
4.4.2	Analysis under varying T condition.....	52
4.5	MPPT performance comparison.....	53
4.5.1	Performance under varying S condition.....	53

Table of contents

4.6. Conclusion.....	54
General conclusion.....	55
References.....	56

List of figures

List of figures:

Fig 1.1: Photovoltaic cells, modules, panel and arrays	4
Fig 1.2: Solar PV system connected to load.....	5
Fig 1.3: solar cell.....	6
Fig 1.4: ideal model.....	7
Fig 1.5: Single-diode R_s model of PV cell	7
Fig 1.6: Single-diode R_p - R_s model.....	8
Fig 1.7: Equivalent circuit of two diodes solar cell.....	8
Fig 1.8: I-V characteristics of PV device	9
Fig 1.9: The Effect of irradiance on I-V curve of PV module.....	10
Fig 1.10: The Effect of irradiance on P-V curve of PV module.....	10
Fig 1.11: Output I-V characteristics of the PV module with different temperature	11
Fig 1.12: Output P-V characteristics of the PV module with different temperature	12
.....	
Fig 2.1: Block diagram of a typical MPPT system	14
Fig 2.2: Buck converter circuit diagrams	15
Figure 2.3: Buck converter waveforms	15
Fig 2.4: Boost converter circuit diagram	16
Fig 2.5: Boost converter waveforms.....	17
Fig 2.6: Buck-Boost converter circuit diagram	18
Fig 2.7: Buck-boost waveforms.....	18
Fig 2.8: Waveform of different types of inverter.....	20
Fig 2.9: DC-AC converter.....	20
Fig 2.10: PWM waveform for a standard inverter.....	21
Fig 2.11: Voltage source inverter topology.....	21

List of figures

.....	
Fig 3.1: Configuration of PV system with DDC.....	24
Fig 3.2: Configuration of PV system with DDC and DC bus.....	26
Fig 3.3: Configuration of PV system with DDC and inverter.....	27
Fig 3.4: Configuration of PV system with DDC, inverter and AC bus	28
Fig 3.5: Flowchart of perturb and observe method	38
Fig 3.6: The principle of the ES-VWP.....	41
Fig 3.7: Flowchart of ES-VWP.....	41
.....	
Fig 4.1: C_R -S curve.....	44
Fig 4.2: C_R -T curve	44
Fig 4.3: C_C -S curve	45
Fig 4.4: C_C -T curve	45
Fig 4.5: P_o -D curve of PV-buck system.....	47
Fig 4.6: P_o -D curve of PV-boost system	47
Fig 4.7: P_o -D curve of PV-buck-boost system.....	47
Fig 4.8: P_o -D curve of PV-buck-DC system.....	47
Fig 4.9: P_o -D curve of PV-boost-DC system	48
Fig 4.10: P_o -D curve of PV-buck-boost-DC system	48
Fig 4.11: P_o -D curve of PV-buck-INV system.....	49
Fig 4.12: P_o -D curve of PV-boost-INV system	49
Fig 4.13: P_o -D curve of PV-buck-boost-INV system	49
Fig 4.14: P_o -D curve of PV-buck-INV-AC system.....	50
Fig 4.15: P_o -D curve of PV-boost-INV-AC system.....	50
Fig 4.16: P_o -D curve of PV-bucks-boost-INV-AC system	50

List of figures

Fig 4.17: Simulation results of duty cycles.....	53
Fig 4.18: Simulation results of output powe.....	54

List of tables

List of tables:

Table 1: The upper and the lower boundaries of MPPYCC for all PV systems	46
Table 2: Results under different irradiance condition.....	51
Table 3: Results under different temperature conditions.....	52
Table 4: Results of Fig 4.18 and Fig 4.17.....	54

Nomenclature

Nomenclature:

MPPT	Maximum power point tracking
MPPTCC	MPPT constraint conditions
MPP	Maximum power point
MPPs	Maximum power points
PWM	Pulse-width modulation
SPWM	Sine-wave pulse-width modulation
PV	Photovoltaic
FPPV	Four-parameter model of PV cell
P&O	perturbation and observation
AC	Alternating current
DC	Direct current
STC	Standard test conditions
DDC	DC/DC converter
BuDDC	Buck DC/DC converter
BoDDC	Boost DC/DC converter
BBDDC	Buck/boost DC/DC converter
D	Duty cycle
D_L	Lower boundary of D in practical application
D_U	Upper boundary of D in practical application
M	Modulation ratio
D_{max}	D at MPP
R_s	PV model Series resistance
R_L	Equivalent load resistance
I_{sc}	Short circuit current of PV cell at STC
V_{oc}	Open circuit voltage of PV cell at STC
I_m	MPP current of PV cell
V_m	MPP voltage of PV cell at STC
V	Output voltage of PV cell
I	Output current of PV cell

Nomenclature

V_o	Output voltage of the DC/DC converter
I_o	Output current of the DC/DC converter
V_r	RMS value of the output voltage of the inverter
I_r	RMS value of the output current of the inverter
P_o	Output power of PV system
$P_{o\max}$	Ideal maximum value of P_o
V_{Abus}	Voltage of the AC bus
V_{Dbus}	Voltage of the DC bus
S	Solar irradiance
T	Cell temperature
VWP	Variable weather parameter
ES-VWP	Equation solution VWP

General introduction

General introduction

We are living in an era where energy security faces multiple threats; the oil spike is signaling an end to energy security, while geo-political instabilities are pushing even the most powerful nations to search for local energy solutions. One obvious consequence of this change is the Global drive toward renewable energy options. Solar energy is considered to be one of the most reliable and promising source of renewable energy, since the Earth receive huge amount of energy which is 1.74×10^{17} watts hours from the sun[1].

Photovoltaic technology is undergoing development in two specific ways: cell material and power conditioner (DC/DC or DC/AC converters) technology, with the objective to increase overall conversion efficiency. The theory about photovoltaic is very important; whether it is for educational or technical purposes; it is a key aspect in improving the quality of energy obtained from PVs. PV arrays have non-linear I-V characteristics and output power depends on atmospheric conditions. There exists only one point named maximum power point MPP on the P-V curve that is on the knee, where power is maximum. MPPT is a technique employed to extract maximum power available from the PV source.

Modeling gives large insights in terms of design and performance assessment. Many models have been proposed; Single and double-diode models have been widely used.

In this report , the single-diode model with four parameters is used, which is beneficial for the hardware design and theoretical research, to look for the existence of the MPPs of 12 configurations, we can estimate by this work, whether PV system can operate or not at its MPP, which is beneficial to choose the MPPT circuit, design the MPPT algorithm and estimate the MPPT effect .Furthermore, the MPPTCC (maximum power point tracking constraint condition) accuracy will be testified on 12 different PV systems under ideal conditions.

Moreover, a novel Variable Weather Parameter (ES-VWP) approach has been developed in this work as an efficient analytical MPPT algorithm. The approach which has been examined in [2][3], and proved to be faster than other classical techniques, was further improved in this project. In essence, the introduced ES-VWP approach relies on IV characteristics of the PV system and attempts to extract closed form equations for Maximum Power Point Tracking.

The remainder of this report is organized as follows:

General introduction

In chapter 1, a general overview on PV systems and their characteristics is provided. Chapter 2 elaborates on DC-DC and DC-AC converters as well as the design procedure. The design and analysis of the proposed MPPT approach as well as its mathematical foundations are laid out in details along chapter 3. The designed approach is then testified through simulation assessments in chapter 4. The report then culminates with a conclusion as well as future work perspectives.

Chapter 1

PV modelling

Chapter 1 : PV modelling

1.1. Introduction

Photovoltaics offer consumers the ability to generate electricity in a clean, quiet and reliable way. Photovoltaic systems are comprised of photovoltaic cells that convert light energy directly into electricity. Because the source of light is usually the sun, they are often called solar cells. The word photovoltaic comes from “photo,” meaning light, and “voltaic,” which refers to producing electricity. Therefore, the photovoltaic processes “producing electricity directly from sunlight.”

1.2. Solar Photovoltaic system:

Solar PV systems are power systems that convert sunlight into electricity by utilizing the photovoltaic effect. This is a process in which semiconducting materials generate voltage and current when exposed to light. For real world applications, this effect is usually implemented with the aid of solar cells which are individual devices whose electrical characteristics vary when exposed to light. These cells are usually made out of polycrystalline or monocrystalline silicon and can be connected in series or parallel to achieve the desired voltage and current respectively. A number of solar cells packed into a metal frame is called a solar module or solar panel and this is the form in which solar PVs are commercially made available for use.

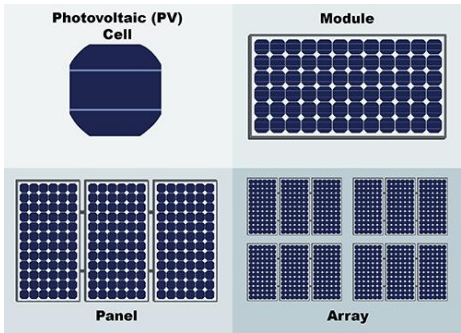


Fig1.1. Photovltaic cells,modules,panels and arrays.

In a solar PV system, the solar panel serves as the receptacle for sunlight and converts the incident photons to electric power. The energy produced by the panel is then converted from direct current (DC) to alternating current (AC) using a solar inverter. Other peripherals include: a solar tracking system to enhance the overall performance and a battery bank for storing the

Chapter 1 : PV modelling

power output. All components of a PV system besides the solar panels are often referred as the balance of system. Solar PV systems can vary in size; from small roof-mounted installation of several megawatts by utilizing large arrays of solar panels. Fig1.2 shows the increasing complexity of a solar PV cell and the constituent devices of a functional solar PV system.

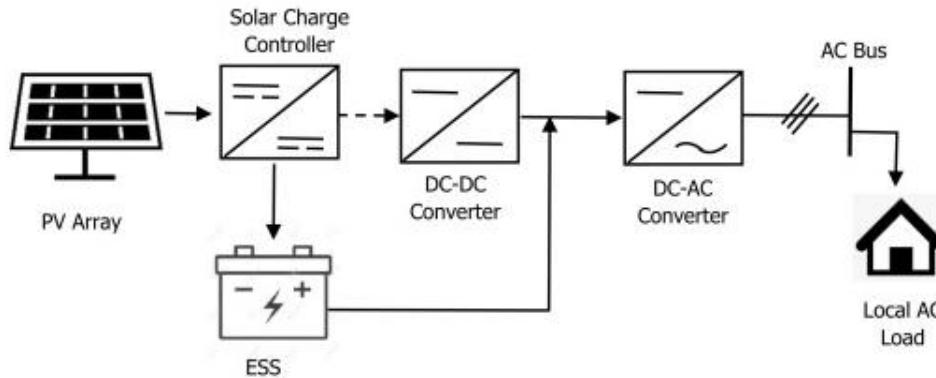


Fig1.2. Solar PV system connected to load.

Currently, due to global transition to clean energy and reduction in carbon emissions, photovoltaic systems have experienced enormous growth and have established themselves as a ripe technology for electricity generation. A roof mounted photovoltaic system recovers the energy invested in its manufacturing within 0.7-2 years and produces approximately 95% clean energy during a 30-years' service life [4].

1.2.1. Structure of a photovoltaic cell

PV cells convert sunlight directly into electricity without creating any air or water pollution. They are made of at least two layers of semiconductor material, one layer has a positive charge, the other has a negative charge. When light enters the cell, some of the photons from the light are absorbed by the semiconductor atoms, freeing electrons from the cell's negative layer to flow through an external circuit and back into the positive layer. This flow of electrons produces electric current. To increase their utility, tens of individual PV cells are interconnected together in a sealed weatherproof package called a module. When two modules are wired together in series, their voltage is doubled while the current stays constant. When two modules are wired in parallel, their current is doubled while the voltage stays constant. To achieve the desired voltage and current, modules are wired in series and in parallel which is called PV array. The flexibility of the modular PV system allows designers to create a solar power system that can meet a variety of electrical needs.

Chapter 1 : PV modelling

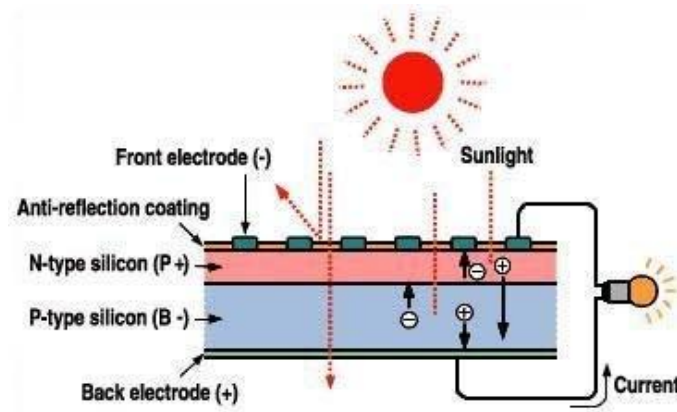


Fig1.3 Solar cell

1.3. Equivalent circuit of a solar cell

The ability to model PV device outputs is key to the analysis of PV system performance. A PV cell is traditionally represented by an equivalent circuit composed of a current source, one or two anti-parallel diodes (D), with or without an internal series resistance (R_s) and a shunt/parallel resistance (R_p). The equivalent PV cell electrical circuits based on the ideal model, a one-diode model and a two-diode model.

1.3.1. Ideal modal

As represented in fig1.4, the ideal PV cell model has the simplest form since it takes no account of the effect of internal electrical series resistances and parallel resistance. The ideal mathematical model for an individual PV cell is expressed as:

$$I = I_{ph} - I_D = I_{ph} - I_0(e^{\frac{V}{V_t}} - 1) \quad (1-1)$$

Where:

$$V_t = \frac{nKT}{q} \quad (1-2)$$

Chapter 1 : PV modelling

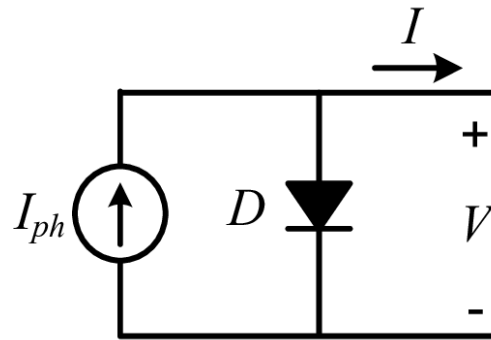


Fig1.4 Ideal model

1.3.2. One-diode model taking account only of R_s (4-p model)

Fig1.3.2 illustrates the equivalent PV cell electrical circuit for series resistance case.

Its mathematical model is presented as:

$$I = I_{ph} - I_D = I_{ph} - I_o \left(e^{\frac{V+IR_s}{V_t}} - 1 \right) \quad (1-3)$$

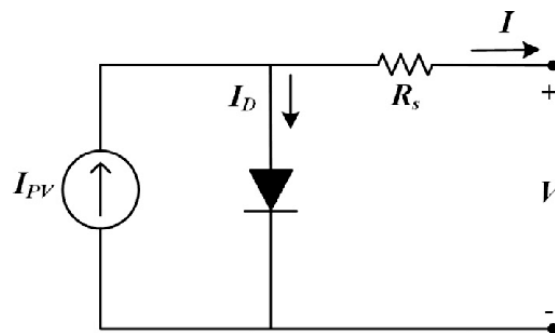


Fig1.5 The single diode R_s -model of PV cell.

1.3.3. One-diode model considering R_s and R_p (5-p model)

To improve the accuracy of the simulation model, parallel resistance is thus introduced in the one- diode model. This is the well-known five parameter model, shown in fig1.3.4 and represented by equation (1.4):

$$I = I_{ph} - I_p - I_D = I_{ph} - I_o \left(e^{\frac{V+IR_s}{V_t}} - 1 \right) - \frac{V+IR_s}{R_p} \quad (1-4)$$

Chapter 1 : PV modelling

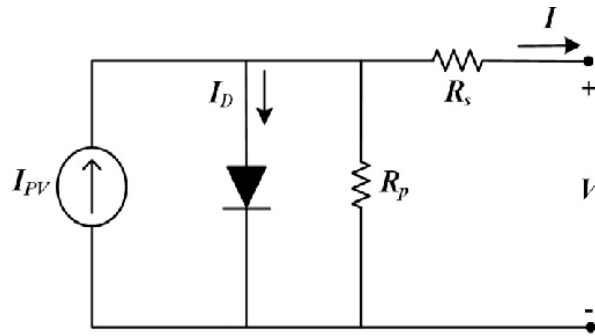


Fig1.6 Single diode Rp-Rs model

1.3.4. Two-diode model

The commonly used one-diode model can achieve acceptable accuracy, but the reality is that the saturation current of the PV cell is the result of a linear superposition of charge diffusion and recombination in the space-charge layer [5]. This means that the saturation current is contributed by two Shockley terms. Therefore, the two diode model was proposed [6-7]. The schematic diagram of the of the equivalent electrical circuit is illustrated in fig 1.3.5 and the mathematical model is expressed as:

$$I = I_{ph} - I_{D1} - I_{D2} - I_p = I_{ph} - I_{D1} \left(e^{V + \frac{IR_s}{R_p}} - 1 \right) - I_{D2} \left(e^{V + \frac{IR_s}{R_p}} - 1 \right) - \frac{V + IR_s}{R_p} \quad (1-5)$$

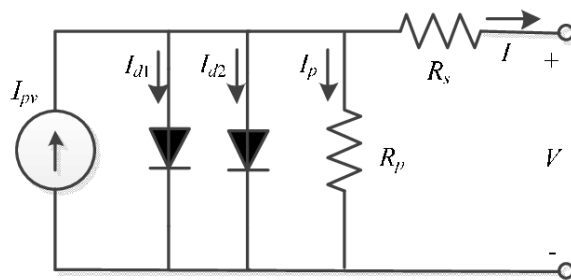


Fig1.7 Equivalent circuit of two diodes solar cell.

1.4. Open Circuit Voltage, Short Circuit Current and Maximum Power Point

The current- voltage(I-V) characteristic is the basic descriptor of photovoltaic device performance. A fundamental understanding of how solar irradiance, cell temperature and

Chapter 1 : PV modelling

electrical load affect I-V curves is essential in designing, installing and evaluating PV system applications.

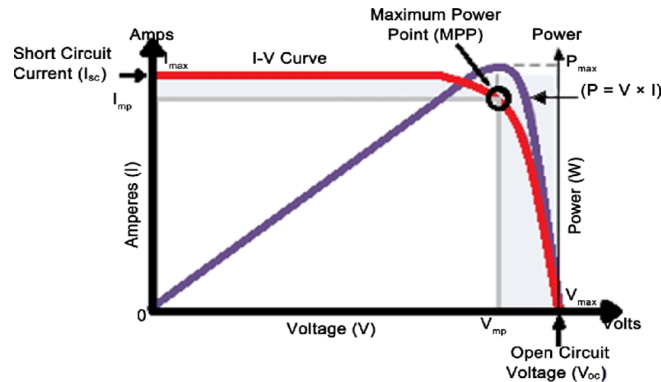


Fig1.8 I-V characteristics for PV device.

- **Open circuit voltage (V_{oc}):** when zero load is connected to PV device (resistance = infinite), a PV device produces maximum voltage and zero current, referred to as its open circuit voltage, V_{oc} .
- **Short circuit current (I_{sc}):** when zero load is connected to a PV device (resistance=zero),the device produces maximum current and zero voltage, referred to as its short circuit current (I_{sc}).
- **Maximum power point (P_{max}):** It is the condition under which the solar cell generates its maximum power. The current and voltage in this condition are defined as I_{mp} and V_{mp} , respectively.
- **The fill factor (FF):** It represents the degree to which the voltage at the maximum power point (V_m) matches the open circuit voltage (V_{oc}) and that the current at the maximum power point (I_m) matches the short circuit current (I_{sc}): The fill factor is calculated using the following formula:

$$FF = \frac{V_{mp} \times I_{mp}}{V_{oc} \times I_{sc}} \quad (1-6)$$

- **Conversion efficiency (η):** It is the maximum percentage of power that can be converted (from absorbed light to electrical energy) and collected when a solar cell is connected to an electrical circuit. It is the ratio of P_{max} to the product of the input light irradiance and the solar cell surface area.

$$\eta = \frac{P_{max}}{P_{in}} \quad (1-7)$$

1.5. Temperature and Irradiance Effect

Chapter 1 : PV modelling

The temperature and irradiance strongly affect the characteristics of solar modules these two parameters vary according to the different seasons over the year and the location of the pv system.

1.5.1. Effect of irradiance

Irradiance play an important role for the performance of any PV system. when all parameters are constant, the higher the irradiance, the greater the output current, and as a result, the greater the power generated. Figure 1.7 shows the relationship between the PV module voltage and current at different solar irradiance levels. The image illustrates that as irradiance increases, the module generates higher current on the vertical axis. Similarly, the voltage and power relationship of PV module at different irradiance levels can be observed. As the irradiance increases, the module is able to generate more power represented by higher peaks on the curves in Fig 1.8.

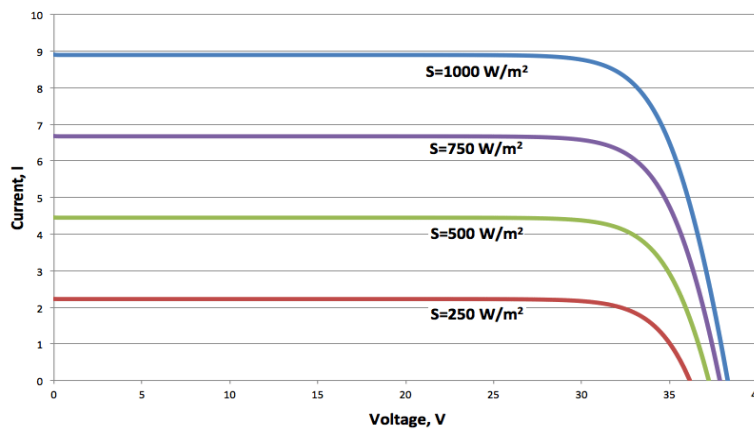


Fig1.9 The effect of irradiance on I-V curve of PV module.

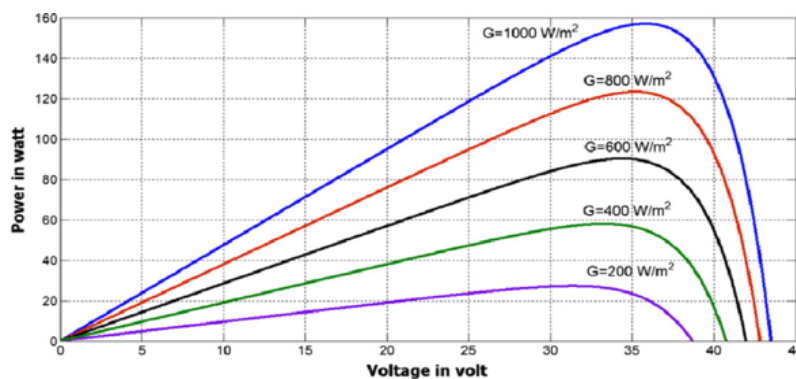


Fig1.10 The effect of irradiance on P-V curve of PV module.

Chapter 1 : PV modelling

1.5.2. Effect of temperature

A PV module's temperature has a great effect on its performance. As can be seen from Fig 1.11 and Fig 1.12, the temperature mainly effects the open circuit voltage; the temperature and open circuit voltage are inversely proportional to each other.

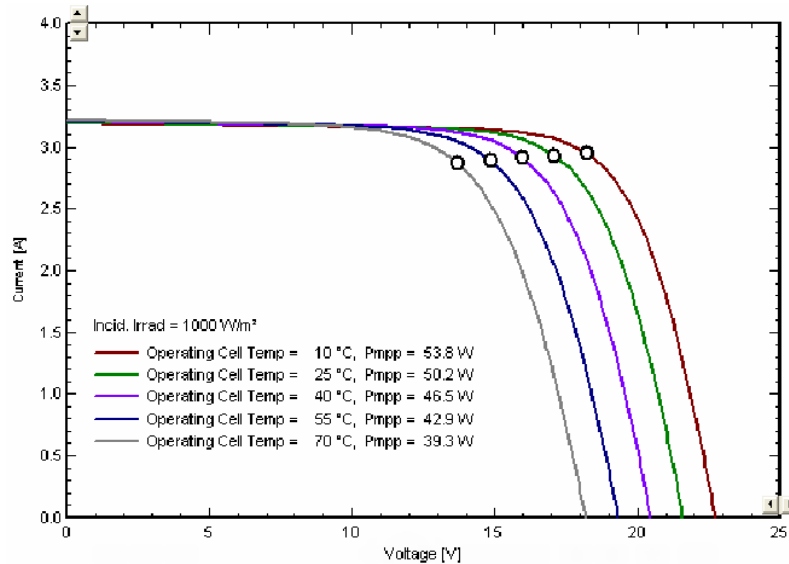


Fig1.11 Output I-V characteristics of the PV module with different temperature.

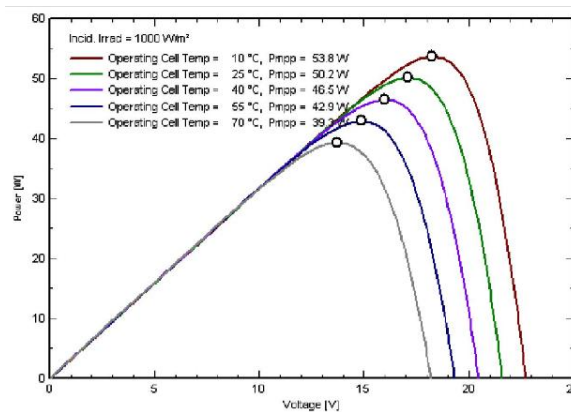


Fig1.12 Output P-V characteristics of the PV module with different temperature.

In general, a crystalline silicon Module's efficiency will be reduced about 0.5 percent for every degree (1°C) increase in temperature. The effect of varying temperature does not have a very large effect on the current developed [6].

Chapter 1 : PV modelling

1.6. Conclusion:

this chapter has covered the modeling of the PV system using different equivalent circuits, we have seen also that the I-V characteristics of the PV module exhibit a nonlinear characteristic. The amount of the power that can be extracted depends on the temperature and radiation. The power produced from the PV panel is directly proportional to the irradiance and inversely proportional to the temperature, for each value temperature and radiation have different maximum power operating points. This MPP is tracked on permanent basis for a given radiation and temperature, in order to track this MPP different algorithm and methods are used which will be discussed in the following chapter.

Chapter2: Converters

Chapter2 :Converters

2.1. Introduction

One of the most important parts in PV system architecture is the power converters. The reason is that they play an important role in transforming the different types of electricity, to make the electricity convenient to the end users. Since the solar cell produces a DC type of electricity, there is room for various types of power converters. Some of the most commonly used power converter types are briefly describing according to their topology, function, efficiency. Since the efficiency of the PV cell is low (around 13%), MPPT are used to extract a maximum possible output power. A dc/dc converter acts as an interface between the load and the module as we can see in Fig 2.1.

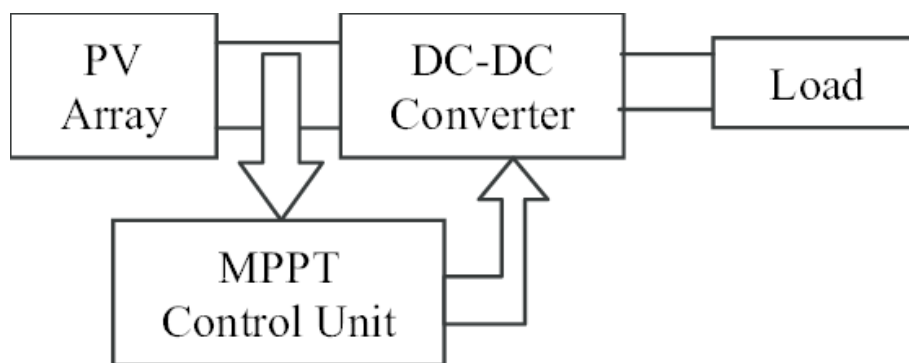


Fig2.1 Block diagram of a typical MPPT system.

2.2.DC-DC CONVERTERS

A dc-dc converter is an electrical system (device) which converts direct current (DC) sources from one voltage level to another. They are used to increase or decrease the voltage level. There are a different types of dc-dc converters, and the most important are: boost converter, buck converter,buck-boost converter.

2.2.1. Buck converter (Step down converter)

It is a DC/DC switch mode power supply that is intended to buck (or lower) the input voltage of an unregulated DC supply to a stabilized lower output voltage. A basic buck converter is shown in Fig.2.1(a).When switch (S) is turned on Fig.2.1(b) current begins flowing through S and L, and then into C and the load, charging the inductor by increasing its magnetic field and increasing V_o Diode D will be on reverse bias, thus blocking the path for current[7].When switch S is turned off Fig.2.1(c) the inductor acts as a source and maintain the current through the load resistor. During this period, the energy stored in the inductor decreases and its current falls. Current continues to flow in the inductor through the diode D as the magnetic field

Chapter2 :Converters

collapses and the inductor discharge. Before the inductor completely discharges, diode D is open and S is closed and the cycle repeats [7]

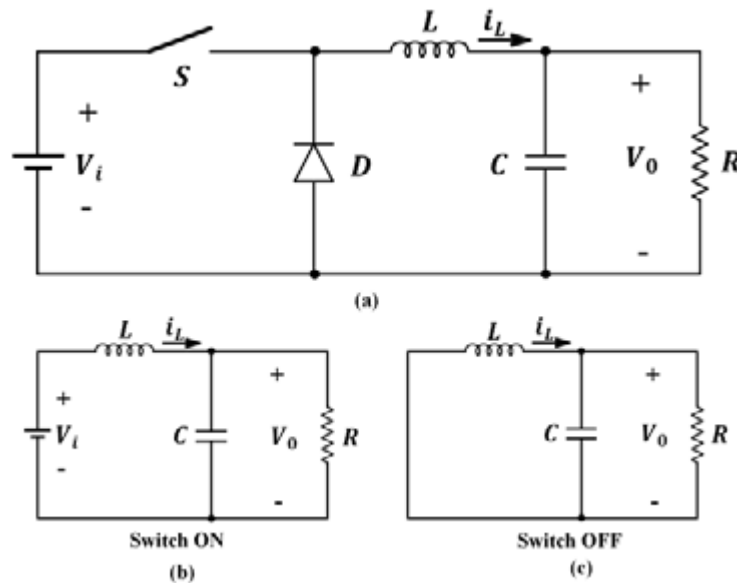


Fig.2.2. (a) Buck converter circuit diagrams

(b) ON state equivalent circuit (c) OFF state equivalent circuit

The waveforms for the switch state , valtage and current are shown in **Fig.2.2**

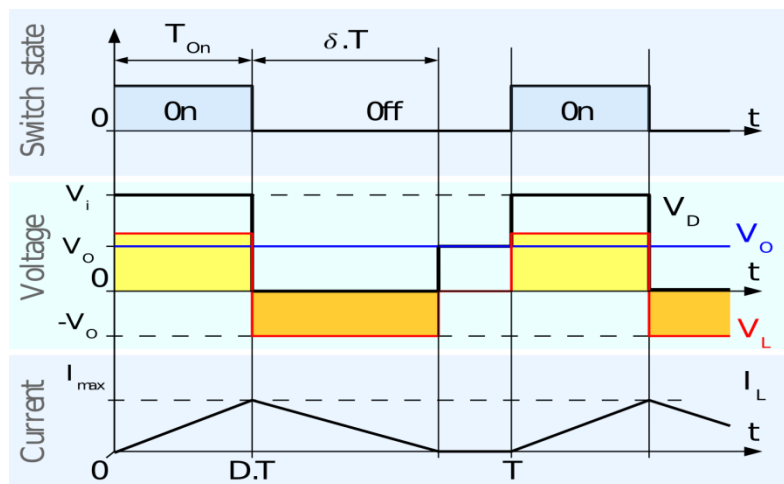


Fig.2.3 Buck converter waveforms.

The average output voltage and current are given by:

$$V_o = DV_i \quad (2.1)$$

$$I_o = \frac{I_i}{D} \quad (2.2)$$

Chapter2 :Converters

The duty cycle of the buck converter is defined as:

$$D = \frac{T_{on}}{T_{on}+T_{off}} \quad (2.3)$$

$$\Delta I = \frac{V_i \cdot D(1-D)}{fL} \quad (2.4)$$

$$\Delta V = \frac{\Delta I}{8fC} = \frac{V_i \cdot D(1-D)}{8f^2CL} \quad (2.5)$$

The critical value for a continuous inductor current and capacitor voltage are:

$$L_C = L = \frac{(1-D)R}{2f} \quad (2.6)$$

$$C_C = C = \frac{1-D}{16Lf^2} \quad (2.7)$$

2.2.2.Boost converter (step up converter)

It is a DC/DC switch mode power supply that is intended to boost (or increase) the input voltage of an unregulated DC supply to a stabilized higher output voltage. Similar to a buck converter, a boost converter relies on an inductor , diode, capacitor , and power switch regulate the output voltage. The Fig2.3(a) shows the basic boost converter. The circuit operation can be divided into two modes, mode(1) begins when switch is closed for time t_1 (t_{on}), as a result the inductor current rises and energy is stored in the inductor L. Mode(2) begins when the switch is opened at time t_2 (t_{off}), the energy stored in the inductor transferred to the load.

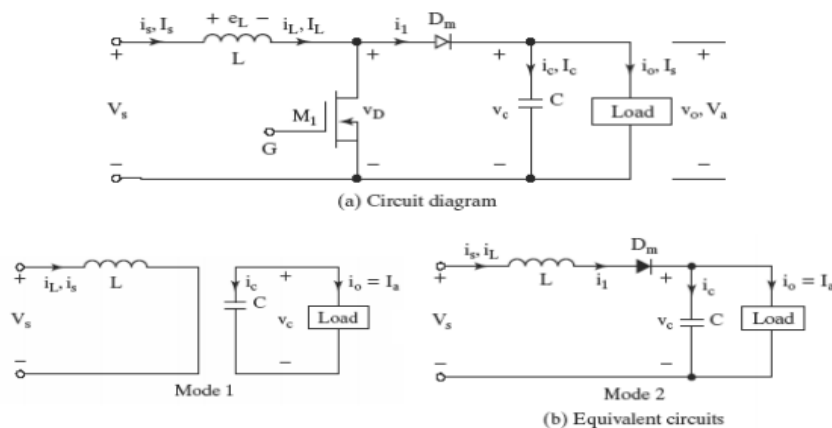


Fig.2.4 (a) Boost converter circuit diagram

(b) Mode1: ON state equivalent circuit (b) Mode 2: OFF state equivalent circuit

Chapter2 :Converters

Assuming a continuous current flow, the waveforms for the switch state, voltage and current are shown in Fig.2.4

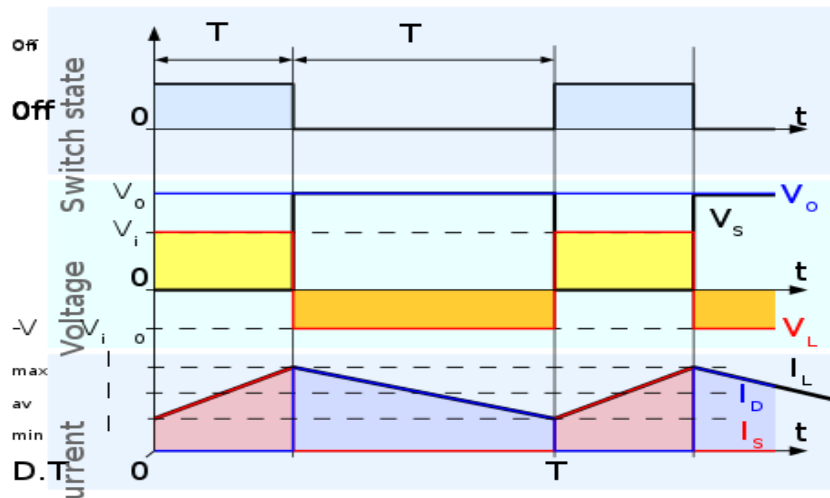


Fig.2.4 Boost converter waveforms.

When the converter is turned on, the voltage across the inductor is:

$$V_l = L \frac{di}{dt} \quad (2.8)$$

And the peak-to-peak ripple current is:

$$\Delta I = \frac{V_s}{L} t_1 \quad (2.9)$$

The average output voltage and current of the boost converter are given by:

$$V_o = \frac{V_i}{1-D} \quad (2.10)$$

$$I_o = I_i(1-D) \quad (2.11)$$

$$\Delta V_C = \frac{I_o(V_o - V_s)}{V_o f C} = \frac{I_a D}{f C} \quad (2.12)$$

The critical values for a continuous inductor current and capacitor:

$$L_C = L = \frac{D(1-D)R}{2f} \quad (2.13)$$

$$C_c = C = \frac{D}{2fR} \quad (2.14)$$

2.2.3. Buck-Boost converter (step down-step up converter)

Chapter2 :Converters

The buck-boost converter is one of the types of chopper, which is a device that convert the DC source into DC output. It can raise or lower the magnitude of input voltage based on the value of duty cycle ratio. The basic circuit of buck-boost converter consists of a diode (D), an inductor (L), and a capacitor (C), switch (generally we use MOSFET) and the load, as we can see in the Fig.2.5(a). When the switch is ON and the diode is OFF, the current flows from the source to the inductor. That is, the inductor gets charged during this condition. The terminals of the inductor gets reversed when the switch is turned OFF and it supplies the energy (current) to the load. When the switch is OFF and the diode is ON, the inductor reverses its terminals and it supplies the stored energy to the load, as a result the inductor discharges its energy to the load.

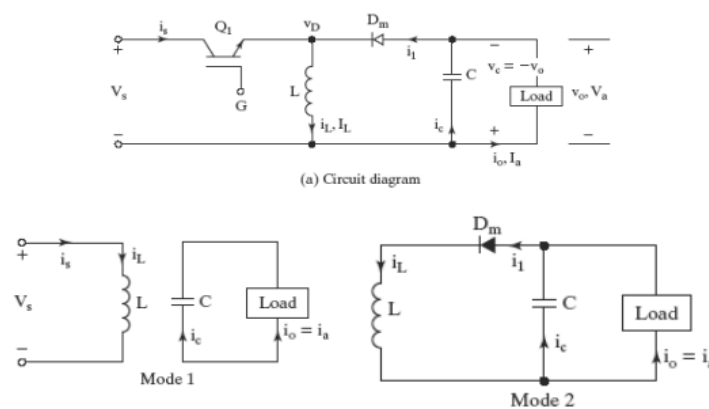


Fig.2.5 (a) Buck-Boost converter circuit diagram

Mode1:ON state equivalent circuit

Mode2:OFF state equivalent circuit.

The waveforms for the switch state, voltage and current are shown in **Fig.2.6**

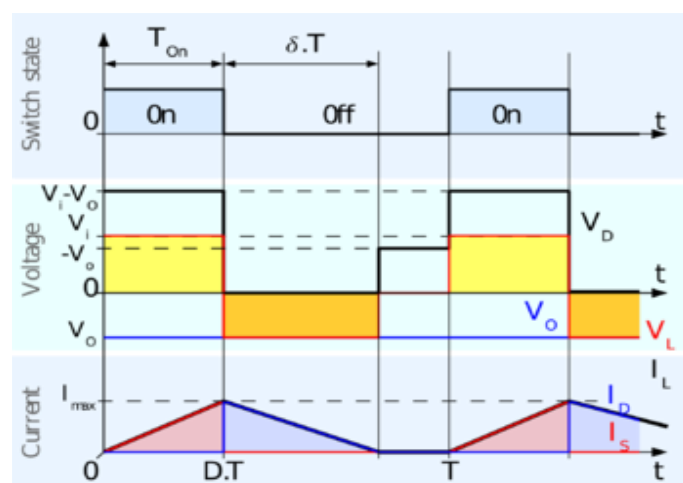


Fig.2.6 Buck-Boost waveforms

Chapter2 :Converters

The average output voltage and current of the buck-boost converter are given by:

$$V_o = \frac{DV_i}{1-D} \quad (2.15)$$

$$I_o = \frac{1-D}{D} I_i \quad (2.16)$$

$$\Delta I = \frac{V_s D}{fL} \quad (2.17)$$

$$\Delta V_C = \frac{I_o V_o}{(V_a - V_s) fC} = \frac{I_o D}{fC} \quad (2.18)$$

The critical values for a continuous inductor current and capacitor voltage:

$$L = \frac{D(1-D)R}{2f} \quad (2.19)$$

$$C = \frac{D}{2fR} \quad (2.20)$$

2.3.DC-DC Converter for a PV application

In PV system, the buck converter is used for wide applications like charging batteries or pumping system, since it provides lower output voltage compared to the input voltage. A buck converter can function at the MPP under most conditions, but it can not operate when the MPP fall under battery charging voltage or low irradiance or high temperature condition. So an additional boost capability can be used to enhance the overall efficiency [8]. The boost converter allow us to track the MPP under low irradiance level or at high temperature since the low voltage of the PV system can be boosted to some required inverter input voltage [9]

2.4.DC-AC converter

The purpose of a DC/AC inverter is to change direct current (DC) electricity into alternating current (AC) electricity. Inverters are needed in PV systems because the electricity generated by the solar panels is DC electricity, and most of electrical devices and household appliances need AC electricity. There is a 3 major types of inverters Fig.2.7: sine wave, Modified sine wave and Square Wave.

Chapter2 :Converters

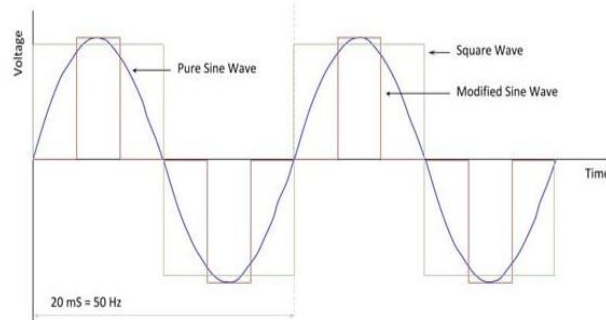


Fig.2.7 Waveform of different types of inverter.[10].

- **Sine wave:** It gives a waveform that we get from hydroelectric power or from a generator.
- **Modified Sine Wave:** actually has a waveform more like a square wave. A lot of equipment work well on modified sine wave inverters, including motors, household appliances and other items.
- **Square wave:** Is very simple, with the dc supply switched between positive and negative.

2.4.1.Steps for DC-AC conversion

Fig2.8.Shows the key components of a DC-AC Converters or inverter.

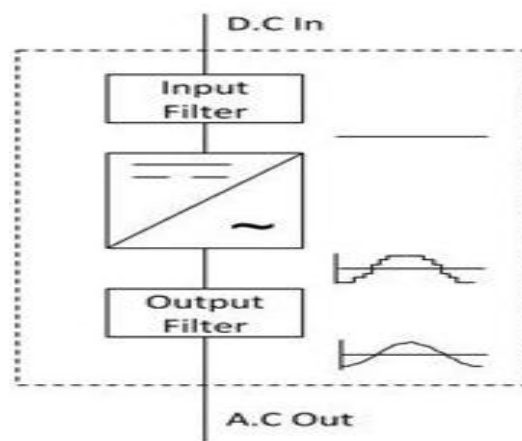


Fig2.8 DC-AC Converter.[10]

- **Input Filter :** It removes any ripple or frequency disturbances on the DC supply to provide a clean voltage to the inverter circuit.
- **Inverter :** Here where the DC in converted into a multiple PWM waveform.
- **Output Filter :** The output filter remove the high frequency components of the PWM wave, to produce a nearly sinusoidal output.

Chapter2 :Converters

2.4.2.Pulse Width Modulation

The most commonly used technique in inverters is called pulse width modulation. Which is used to turn the DC voltage on and off with a certain pulse. The width of each pulse is varied so that the overall electrical result is similar to that of a sine wave.

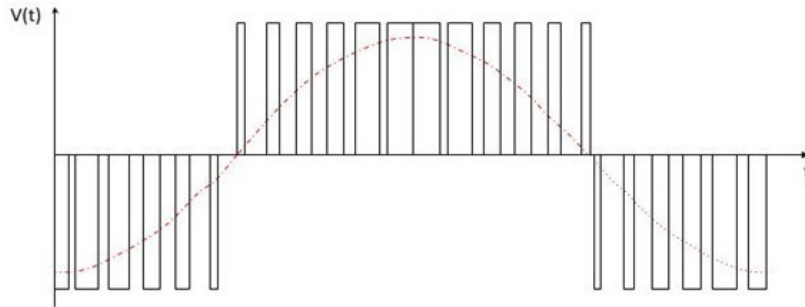


Fig.2.9 PWM weveform for a standard inverter.

A single DC voltage is switched on or off to generate the desired output. More input DC voltage levels are used to create an ouput waveform that more closely resembles a sine wave.

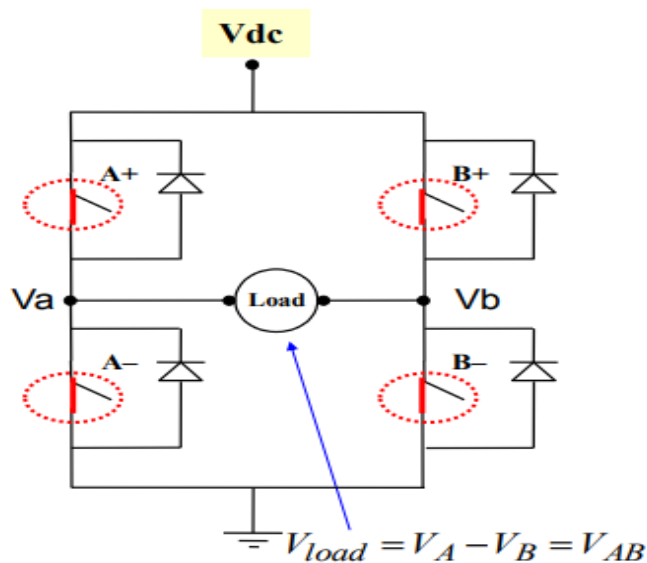


Fig2.10.Voltage source inverter topology.

According to Fig2.10.We can create AC voltage from DC voltage when:

- A^+ closed , $V_a=V_{dc}$.
- A^- closed , $V_a=0$.
- B^+ closed , $V_b=V_{dc}$.
- B^- closed , $V_b=0$.

Chapter2 :Converters

2.5.CONCLUSION

As demenstrated in previous chapter,MPPT tracking is very important to deliver maximum output power to the load and increase the system efficiency. A DC-DC converter is used in pv system across the load and the source to extrect the maximum power transfer between the source and the load.The boost converter is used when the load impedance is lower compared the source impedance.Buck converter is used when the load impedance is higher compared to the source impedance. By changing the duty cycle of the converter for each value of temperature and irradiation.the impedance matching can be reached using MPPT algorithms and that will be investigated in the following chapter.

Chapter3: Maximum Power Point Tracking Constraint conditions

Maximum Power Point Tracking Constraint conditions

3.1.Introduction

The maximum power point (MPP) may be not tracked successfully because of the constraint conditions among some circuit parameters. In this chapter a maximum power point tracking (MPPT) constraint conditions of photovoltaic (PV) system with different configurations are found by analyzing their integrated mathematical models. Based on them, a variable-weather-parameter (VWP) MPPT control strategy is proposed. By the use of it, the complex control of the system will be avoided, which ensured the lower hardware cost, shorter design period and better MPPT performance.

3.2.Integrated modeling of PV system

3.2.1.PV system with DDC

The configuration of PV system with the DC/DC converter (DDC) can be shown in Fig.3.1

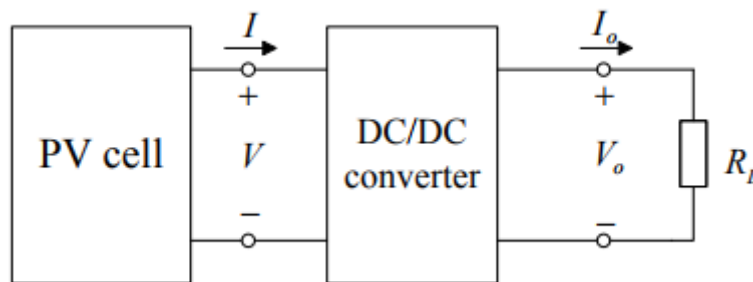


Fig.3.1 Configuration of PV system with DDC.

We know that: $I_{sc} = I_{ph} \text{ \& \ } I_o = I_{sc}e^{-AV_{oc}}$

$$I = I_{ph} - I_o e^{AV} \quad (*)$$

And :

$$\begin{cases} (V = 0, I = I_{sc}) \\ (I = 0, V = V_{oc}) \end{cases}$$

So :

$$I_{sc} = I_o e^{AV_{oc}}$$

$$I_o = I_{sc} e^{-AV_{oc}} \quad (**)$$

In addition :

$$\begin{cases} I_{sc} = I_{ph} \\ I_o = I_{sc} e^{-AV_{oc}} \end{cases}$$

Maximum Power Point Tracking Constraint conditions

We replace all results in (*) :

$$I_m = I_{sc} - I_0 e^{AV_{oc}}$$

$$I_m = I_{sc} - I_{sc} e^{-AV_{oc}} * e^{AV_m}$$

$$I_m = I_{sc} (1 - e^{A(V_m - V_{oc})})$$

$$\frac{I_m}{I_{sc}} = 1 - e^{A(V_m - V_{oc})}$$

$$1 - \frac{I_m}{I_{sc}} = e^{A(V_m - V_{oc})} \rightarrow A \frac{1}{V_m - V_{oc}} * \log\left(1 - \frac{I_m}{I_{sc}}\right)$$

We take :

$$C_1 = \left(1 - \frac{I_m}{I_{sc}}\right) e^{\frac{-V_m}{C_2 V_{oc}}} \quad (3.1)$$

And :

$$C_2 = \frac{\frac{V_m - 1}{V_{oc}}}{\log\left(1 - \frac{I_m}{I_{sc}}\right)} \quad (3.2)$$

So :

$$I = I_{sc} \left[1 - C_1 \left(e^{\frac{-V}{C_2 V_{oc}}} - 1\right)\right] \quad (3.3)$$

The mathematical models of the PV cell, BuDDC, BoDDC, BBDDC, and the load can be expressed by equations (3.1, 3.2, 3.3) [11][12]

$$P_0 = \frac{V_0^2}{R_L} \quad (3.4)$$

For Buck converter and According to equations (3.3) and (2.1) and (3.4) we have:

$$P_0 = \frac{R_L I_{sc}^2}{D^2} \left[1 - C_1 \left(e^{\frac{\sqrt{P_0 R_L}}{C_2 V_{oc} D}} - 1\right)\right]^2 \quad (3.5)$$

The integrated mathematical model of PV system with BoDDC by using equations (3.3 , 2.10 and 3.4) we get :

$$P_0 = R_L I_{sc}^2 (1 - D)^2 \left[1 - C_1 \left(e^{\frac{\sqrt{P_0 R_L} (1-D)}{C_2 V_{oc}}} - 1\right)\right]^2 \quad (3.6)$$

And the integrated mathematical model of PV system with BBDDC can be expressed as :

$$P_0 = \frac{R_L I_{sc}^2 (1-D)^2}{D^2} \left[1 - C_1 \left(e^{\frac{\sqrt{P_0 R_L} (1-D)}{C_2 V_{oc} D}} - 1\right)\right]^2 \quad (3.7)$$

Maximum Power Point Tracking Constraint conditions

3.2.2.PV system with DDC and DC bus

The configuration of PV system with DDC and DC bus can be shown by the Fig.3.2.

The mathematical model of the DC bus can be represented by equation (3.8).

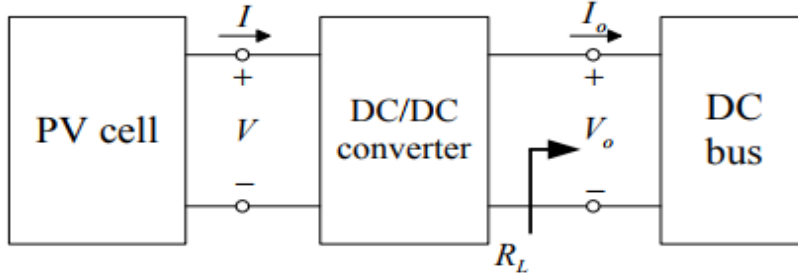


Fig.3.2 Configuration of PV system with DDC and DC Bus.

To make the analysis simpler , we assume the voltage value of the DC bus is constant:

$$V_o = V_{Dbus} \quad (3.9)$$

According to Eq (3.3) , Eq(2.1) and Eq(3.9) , the integrted model of PV system with BuDDC and DC bus can be expressed as :

$$P_o = \frac{V_{Dbus} I_{sc}}{D} [1 - C_1 (e^{\frac{V_{Dbus}}{C_2 V_{oc} D}} - 1)] \quad (3.10)$$

In addition , according to Eq (3.3) ,Eq (2.10) and (3.9) , the integrated mathematical model of PV system with BoDDC and DC bus can be expressed as :

$$P_o = V_{Dbus} I_{sc} (1 - D) [1 - C_1 \left(e^{\frac{V_{Dbus}(1-D)}{C_2 V_{oc}}} - 1 \right)] \quad (3.11)$$

And according to Eq (3.3) , Eq (2.15) and (3.9), the integrated mathematical model with BBDDC and DC bus is :

$$P_o = \frac{V_{Dbus} I_{sc} (1-D)}{D} [1 - C_1 \left(e^{\frac{V_{Dbus}(1-D)}{C_2 V_{oc} D}} - 1 \right)] \quad (3.12)$$

3.2.3.PV system with DDC and inverter

Fig 3.3 shows the configuraion of PV system with DDC and inverter.

Maximum Power Point Tracking Constraint conditions

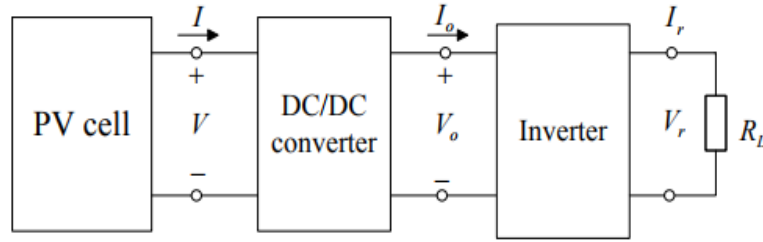


Fig.3.3 Configuration of PV system with DDC and inverter.

We know that :

$$V_r = \frac{MV_o}{\sqrt{2}} \quad (3.13)$$

M: is the modulation index.

$$R_L = \frac{V_r}{I_r} \quad (3.14)$$

For PV system with BuDDC and inverter, according to Eq(3.3),Eq(2.10) , Eq(3.13) and Eq (3.14) we get:

$$P_o = \frac{2R_L I_{sc}^2}{D^2 M^2} [1 - C_1 (e^{\frac{\sqrt{2P_o R_L}}{C_2 V_{oc} D M}} - 1)]^2 \quad (3.15)$$

And for BoDDC and inverter the integrated mathematical model of PV system ,according to Eq (3.3) ,Eq (2.15) , Eq (3.13) and Eq (3.14) we have :

$$P_o = \frac{2R_L I_{sc}^2 (1-D)^2}{M^2} [1 - C_1 \left(e^{\frac{\sqrt{2P_o R_L} (1-D)}{C_2 V_{oc} M}} - 1 \right)]^2 \quad (3.16)$$

According to Eq (3.3), Eq (2.15) ,Eq (3.13) and (3.14) , the intgrated mathematical model of PV system with BBDDC and inverter is :

$$P_o = \frac{2R_L I_{sc}^2 (1-D)^2}{D^2 M^2} [1 - C_1 (e^{\frac{\sqrt{2P_o R_L} (1-D)}{C_2 V_{oc} D M}} - 1)]^2 \quad (3.17)$$

3.2.4.PV system with DDC , Inverter and AC bus

The AC bus is connected with the inverter as can be seen in Fig .3.4

Maximum Power Point Tracking Constraint conditions

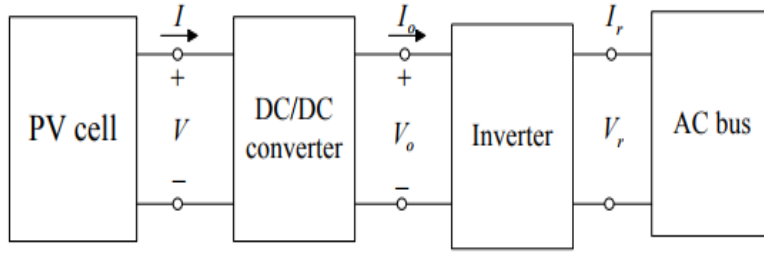


Fig.3.4 Configuration of PV system with DDC , inverter and AC bus.

The mathematical model of the AC bus can be represented by Eq (3.18)

$$V_r = V_{Abus} \quad (3.18)$$

To make the analysis simpler ,we assume the voltage value of AC Bus as a constant.

In case of BuDDC, inverter and AC bus ,and according to Eq(3.3), Eq(2.1) , Eq (3.13) and Eq (3.18) we have:

$$P_o = \frac{\sqrt{2}V_{bus} I_{sc}}{MD} \left[1 - C_1 \left(e^{\frac{\sqrt{2}V_{Abus}}{C_2 V_{ocDM}} - 1} \right) \right] \quad (3.19)$$

For the PV system with BoDDC , inverter and AC bus , and according to Eq(3.3), Eq(2.10) ,Eq (3.13) and Eq(3.18) we have :

$$P_o = \frac{\sqrt{2}V_{bus} I_{sc}(1-D)}{M} \left[1 - C_1 \left(e^{\frac{\sqrt{2}V_{Abus}(1-D)}{C_2 V_{ocM}} - 1} \right) \right] \quad (3.20)$$

And with BBDDC,inverter and AC bus according to Eq(3.3), Eq(2.15) ,Eq (3.13) and Eq(3.18) we have :

$$P_o = \frac{\sqrt{2}V_{bus} I_{sc}(1-D)}{DM} \left[1 - C_1 \left(e^{\frac{\sqrt{2}V_{Abus}(1-D)}{C_2 V_{ocMD}} - 1} \right) \right] \quad (3.21)$$

3.3.MPPTCC under ideal conditions

3.3.1.Expressions of the MPPTCC

Under ideal condition we use Eq(3.22) to analyze MPPTCC.

$$\frac{dP_o}{dD} = 0 \quad (3.22)$$

Maximum Power Point Tracking Constraint conditions

In the first configuration (PV+DDC+ R_L), we replace Eq(3.5),Eq(3.6) and Eq(3.7) in Eq (3.22), and after simplification we get :

$$\text{For PV Buck system: } D_{\max} = \frac{V_{oc\max}}{C} = \frac{\sqrt{P_{o\max}R_L}}{C} \quad (3.23)$$

$$\text{For PV boost system : } D_{\max} = 1 - \frac{C}{\sqrt{P_{o\max}R_L}} \quad (3.24)$$

$$\text{For PV Buck/boost system: } D_{\max} = \frac{\sqrt{P_{o\max}R_L}}{C + \sqrt{P_{o\max}R_L}} = 1 - \frac{C}{C + \sqrt{P_{o\max}R_L}} \quad (3.25)$$

Where C can be expressed as [13] :

$$C = C_2 V_{oc} [\text{lambertw} \left(e^{\frac{1+C_1}{C_1}} \right) - 1] \quad (3.26)$$

$$\text{As known } 0 \leq D \leq 1 \quad (3.27)$$

By Substituting Eq (3.23),Eq(3.24) and Eq(3.25) in Eq (3.27).The MPPTCC of PV-buck system, PV-boost and PV-buck/boost system can be expressed respectively by the following equations:

$$0 \leq R_L \leq \frac{C^2}{P_{o\max}} \quad (3.28)$$

$$\frac{C^2}{P_{o\max}} \leq R_L \quad (3.29)$$

$$0 < R_L \quad (3.30)$$

In the second configuration (PV+DDC+DC bus),we replace Eq(3.10),Eq(3.11) and Eq(3.12) in Eq(3.22) we get:

$$\text{For PV Buck system: } D_{\max} = \frac{V_{D\text{bus}}}{C} \quad (3.31)$$

$$\text{For PV boost system : } D_{\max} = 1 - \frac{C}{V_{D\text{bus}}} \quad (3.32)$$

Maximum Power Point Tracking Constraint conditions

For PV Buck/bost system:
$$D_{\max} = \frac{V_{D_{\text{bus}}}}{C + V_{D_{\text{bus}}}} = 1 - \frac{C}{C + V_{D_{\text{bus}}}} \quad (3.33)$$

Substituting Eq (3.31), Eq(3.32) and Eq(3.33) in Eq(3.27). The MPPTCC of PV-buck system, PV-boost and PV-buck/bost system can be expressed respectively by the following equations:

$$0 < V_{D_{\text{bus}}} \leq C \quad (3.34)$$

$$C \leq V_{D_{\text{bus}}} \quad (3.35)$$

$$0 < V_{D_{\text{bus}}} \quad (3.36)$$

For the third configuration (PV+DDC+INV+Rload), we replace Eq(3.15),Eq(3.16) and Eq(3.17) in Eq(3.22) we get:

For PV Buck system:
$$D_{\max} = \frac{\sqrt{2P_{\text{omax}}R_L}}{C} \quad (3.31)$$

For PV bost system :
$$D_{\max} = 1 - \frac{C M}{\sqrt{2P_{\text{omax}}R_L}} \quad (3.32)$$

For PV Buck/bost system:
$$D_{\max} = 1 - \frac{C M}{C M + \sqrt{2P_{\text{omax}}R_L}} \quad (3.33)$$

Substituting Eq(3.31),Eq(3.32) and Eq(3.33) into Eq(3.27),the MPPTCC of PV-buck-Inv system,PV-bost-Inv system and PV-buck/bost-Inv system can be expressed respectively by:

$$\frac{\sqrt{2P_{\text{omax}}R_L}}{C} \leq M \leq 1 \quad (3.34)$$

$$0 < M \leq \frac{\sqrt{2P_{\text{omax}}R_L}}{C} \quad (3.35)$$

$$0 < M \leq 1 \quad (3.36)$$

So we can deduce the limits of R_L ,according to Eq(3.34) and Eq(3.35) :

$$0 < R_L \leq \frac{M^2 c^2}{2P_{\text{omax}}} \quad (3.37)$$

Maximum Power Point Tracking Constraint conditions

$$R_L \geq \frac{M^2 c^2}{2P_{omax}} \quad (3.38)$$

For the fourth application ,PV-Buck-INV-AC system , PV-boost-INV-AC system and PV-buck/boost-INV-AC system, Equations (3.39),(3.40) and (3.41) can be obtained by substituting Eq(3.19),Eq(3.20) and Eq(3.21) into Eq(3.20) repectively we get:

$$D_{max} = \frac{\sqrt{2}V_{Abus}}{CM} \quad (3.39)$$

$$D_{max} = 1 - \frac{CM}{\sqrt{2}V_{Abus}} \quad (3.40)$$

$$D_{max} = \frac{\sqrt{2}V_{bus}}{CM+\sqrt{2}V_{Abus}} = 1 - \frac{CM}{CM+\sqrt{2}V_{Abus}} \quad (3.41)$$

Substituting Eq(3.39),Eq(3.40) and Eq(3.41) in Eq(3.22) we get :

$$0 < V_{Abus} \leq \frac{CM}{\sqrt{2}} \quad (3.42)$$

$$\frac{CM}{\sqrt{2}} \leq V_{Abus} \quad (3.43)$$

$$V_{Abus} > 0 \quad (3.44)$$

We can select the index M easily from Eq (3.42) and Eq(3.43)

$$\frac{\sqrt{2}V_{Abus}}{C} \leq M \leq 1 \quad (3.45)$$

$$0 < M \leq \frac{\sqrt{2}V_{bus}}{C} \quad (3.46)$$

Under Ideal condition MPPTCC of PV system with different configurations can be clearly shown by the previous equations, these expresions are sufficient and necessary conditions to track the MPP succefully under ideal conditions.

Maximum Power Point Tracking Constraint conditions

We can notice that there is a hardly any constraint conditions for PV-buck/boost system ,PV buck/boost-DC bus,PV buck/boost-Inv system and PV-back/boost-Inv-ACbus system under ideal conditions . by contrast , some constraint condition always exist for other PV system , even if they are ideal circuit.To track MPPT succesfully the MPPTCC corresponding to each configuration must be met.

3.3.2.MPPTCC based on four-parameter model of PV cell

In order to analyze the relationship between four-parameter model of PV cell (FPPV) and MPPTCC we will use Eq(3.47) and Eq(.48) [14]:

$$P_{\text{Omax}} = C_D^2 \frac{C^2}{R_{\text{os}}} \quad (3.47)$$

$$C_D = \sqrt{\frac{1+C_1-C_1 e^{C_{1w}}}{C_2 C_{1w}}} \quad (3.48)$$

Where R_{os} is a virtual resistance of PV cell , and $C_{1w}=\text{lambertw}(e+\frac{e}{C_1}) - 1$.

$$R_{\text{os}} = \frac{V_{\text{oc}}}{I_{\text{sc}}} \quad (3.49)$$

According to Eq(3.47) and Eq(3.49) we have:

$$\frac{C^2}{P_{\text{Omax}}} = C_R \frac{V_{\text{oc}}}{I_{\text{sc}}} \quad (3.50)$$

Where C_R can be expressed by Eq (3.51) :

$$C_R = \frac{1}{C_D} = \frac{C_2 C_{1w}}{1+C_1-C_1 e^{C_{1w}}} \quad (3.51)$$

And according to Eq(3.26) we get :

$$C = C_c V_{\text{oc}} \quad (3.52)$$

Where: $C_c=C_2 C_{1w}$.

Maximum Power Point Tracking Constraint conditions

We substitute Eq(3.50) into Eqs (3.28),(3.29),(3.34),(3.35),(3.37)and (3.38) , then we get the following Equations:

$$0 < R_L \leq C_R \frac{V_{oc}}{I_{sc}} \quad (3.53)$$

$$R_L \geq C_R \frac{V_{oc}}{I_{sc}} \quad (3.54)$$

$$\sqrt{\frac{2R_L I_{sc}}{C_R V_{oc}}} \leq M \leq 1 \quad (3.55)$$

$$1 \leq M \leq \sqrt{\frac{2R_L I_{sc}}{C_R V_{oc}}} \quad (3.56)$$

$$0 < R_L \leq \frac{V_{oc} C_R M^2}{2I_{sc}} \quad (3.57)$$

$$R_L \geq \frac{V_{oc} C_R M^2}{2I_{sc}} \quad (3.58)$$

And we substitute Eq(3.52) into Eqs.(3. 34),(3.35),(3.42),(3.43),(3.45) and (3.46) ,then we get the following Eqs:

$$0 < V_{Dbus} \leq C_c V_{oc} \quad (3.59)$$

$$V_{Dbus} \geq V_{oc} C_c \quad (3.60)$$

$$0 < V_{Abus} \leq \frac{V_{oc} C_c M}{\sqrt{2}} \quad (3.61)$$

$$V_{Abus} \geq \frac{V_{oc} C_c M}{\sqrt{2}} \quad (3.62)$$

3.3.3.MPPTCC in practical application

The parameters C_R and C_c have been successfully expressed by the cell model parameters (V_m, I_m, V_{oc} and I_{sc}) ,the previous MPPTCC from Eq(3.50) til Eq (3.62) based on the cell model parameters are still complex . Therefore, to simplify the expressions of these

Maximum Power Point Tracking Constraint conditions

MPPTCC, C_R and C_C can be assumed as two constants . The DDC and inverter are the non-ideal circuits, therefore these MPPTCC are not available in practical application .It is generally known that the duty cycle can not be too small for the BuDDC while it can not be too big for the BoDDC . In addition , for the BBDDC , its duty cycle can not be too small or too big .Therefore , to find the MPPTCC in practical application , assume that the minimum duty cycle of the BuDDC or BBDDC can be represented by D_L and the maximum duty cycle of the BBDDC can be represented by D_U . Now, Eq(3.63),Eq(3.64),Eq(3.65) can be used for the BuDDC , BoDDC and BBDDC, repectively.

$$D_L < D_{\max} \leq 1 \quad (3.63)$$

$$0 < D_{\max} \leq D_U \quad (3.64)$$

$$D_L < D_{\max} \leq D_U \quad (3.65)$$

For PV-buck system,PV-boost system and PV-buck/boost system, we substitute Eq(3.23),Eq(3.24) and Eq (3.25) into Eq(3.63),Eq(3.64) and Eq(3.65) we get the three DDCs for the MPPTCC of PV.

$$\frac{C^2 D^2 L}{P_{\max}} \leq R_L \leq \frac{C^2}{P_{\max}} \quad (3.66)$$

$$\frac{C^2}{P_{\max}} \leq R_L \leq \frac{C^2 D^2 L}{(1-D_U)^2 P_{\max}} \quad (3.67)$$

$$\frac{C^2 D^2 L}{(1-D_L)^2 P_{\max}} \leq R_L \leq \frac{C^2 D^2 U}{(1-D_U)^2 P_{\max}} \quad (3.68)$$

The MPPTCC of PV system with three DDCs when the MPFPPV is used , the result is given by substituting Eq (3.50) into Eq(3.66), Eq(3.67) and Eq(3.68) ,we get :

$$D^2_L C_R \frac{V_{oc}}{I_{sc}} \leq R_L \leq C_R \frac{V_{oc}}{I_{sc}} \quad (3.66)$$

$$C_R \frac{V_{oc}}{I_{sc}} \leq R_L \leq \frac{V_{oc} C_R}{(1-D_U)^2 I_{sc}} \quad (3.67)$$

$$\frac{C^2 D^2_L C_R}{(1-D_L)^2 I_{sc}} \leq R_L \leq \frac{C_R D^2_U V_{oc}}{(1-D_U)^2 I_{sc}} \quad (3.68)$$

Maximum Power Point Tracking Constraint conditions

Secondly, for PV-buck-DC system, PV-boost-DC system and PV-buck/boost-DC system we substitute Eq(3.31), Eq(3.32) and Eq(3.33) into Eqs(3.63, 3.64, 3.65), we get the three DDCs of DC bus for the MPPTCC of PV system .

$$D_L C \leq V_{D_{bus}} \leq C \quad (3.69)$$

$$C \leq V_{D_{bus}} \leq \frac{C}{1-D_U} \quad (3.70)$$

$$\frac{C D_L}{1-D_L} \leq V_{A_{bus}} \leq \frac{C D_U}{1-D_U} \quad (3.71)$$

Now we substitute Eq(3.52) into Eq(3.69), Eq(3.70) and Eq(3.71). The MPPTCC of PV system with three DDCs and DC bus Equations when the MPFPPV is used

$$D_L C_C V_{oc} \leq V_{D_{bus}} \leq C_C V_{oc} \quad (3.69)$$

$$C_C V_{oc} \leq V_{D_{bus}} \leq \frac{C_C V_{oc}}{1-D_U} \quad (3.70)$$

$$\frac{C_C V_{oc} D_L}{1-D_L} \leq V_{A_{bus}} \leq \frac{C_C V_{oc} D_U}{1-D_U} \quad (3.71)$$

Thirdly, for PV-buck-INV system , PV-boost-INV system and PV-buck/boost-INV system , we substitute Eq(3.31), Eq(3.32) and Eq(3.33) into Eq(3.63), Eq(3.64) and Eq(3.65). eqs (3.72)

And(3.73) and (3.74) can be presented. They are the MPPTCC of the PV system with three DDCs and inverter

$$\frac{C^2 D^2 L M^2}{2 P_{omax}} \leq R_L \leq \frac{C^2 M^2}{2 P_{omax}} \quad (3.72)$$

$$\frac{C^2 M^2}{2 P_{omax}} \leq R_L \leq \frac{C^2 M^2}{2 P_{omax} (1-D_U)^2} \quad (3.73)$$

$$\frac{C^2 D^2 L M^2}{2 P_{omax} (1-D_L)^2} \leq R_L \leq \frac{C^2 M^2 D_U^2}{2 P_{omax} (1-D_U)^2} \quad (3.74)$$

Submitting eq(3-50) into eq(3.72), eq(3.73), eq(3.74), respectively, eq(3.75) and eq(3.76) and eq(3.77) can be given. They are the MPPTCC of PV system with three DDCs and inverter when the MPFPPV is used.

Maximum Power Point Tracking Constraint conditions

$$\frac{CR Voc D^2 L M^2}{2Isc} \leq R_L \leq \frac{M^2 CR Voc}{2Isc} \quad (3.75)$$

$$\frac{CR Voc M^2}{2Isc} \leq R_L \leq \frac{M^2 CR Voc}{2(1-Du)^2 Isc} \quad (3.76)$$

$$\frac{CR Voc M^2 D L^2}{2Isc(1-D)^2} \leq R_L \leq \frac{M^2 CR Voc Du^2}{2(1-Du)^2 Isc} \quad (3.77)$$

Fourthly, for PV-buck-INV-AC system, PV-boost-INV-AC system and PV-buck/boost-INV-AC system, submit eq(3.39) and eq(3.40) and eq(3.41) into eq(3.63), eq(3.64), eq(3.65), respectively, eq(3.78), eq(3.79); eq(3.80) can be presented. They are the MPPTCC of PV system with three DDCs, inverter and AC bus.

$$\frac{C M D_L}{\sqrt{2}} \leq V_{Abus} \leq \frac{C M}{\sqrt{2}} \quad (3.78)$$

$$\frac{C M}{\sqrt{2}} \leq V_{Abus} \leq \frac{C M}{\sqrt{2}(1-Du)} \quad (3.79)$$

$$\frac{C M D_L}{\sqrt{2}(1-D_L)} \leq V_{Abus} \leq \frac{C M Du}{\sqrt{2}(1-Du)} \quad (3.80)$$

submitting eq(3.52) into eq(3.78), eq(3.79), (3.80) can be given. They are the MPPTCC of PV system with three DDCs, inverter and AC bus when the MPFPV is used

$$\frac{D_L M Cc Voc}{\sqrt{2}} \leq V_{Abus} \leq \frac{M Cc Voc}{\sqrt{2}} \quad (3.81)$$

$$\frac{M Cc Voc}{\sqrt{2}} \leq V_{Abus} \leq \frac{M Cc Voc}{\sqrt{2}(1-Du)} \quad (3.82)$$

$$\frac{D_L M Cc Voc}{\sqrt{2}(1-D_L)} \leq V_{Abus} \leq \frac{M Du Cc Voc}{\sqrt{2}(1-Du)} \quad (3.83)$$

In case of an inverter is connected with different DDCs in PV system, its control signal (M) is hardly selected to implement the MPPT control in practical application, therefore for PV-buck-INV system, PV-boost-INV system, PV-buck/boost-INV system, PV-buck-INV-AC system and PV-boost-INV-AC system only some expressions based on R_L , V_{dbus} and V_{abus} are given by previous equations, it is obvious that in practical application, there exist the MPPTCC for PV-

Maximum Power Point Tracking Constraint conditions

buck/boost system PV-buck/boost-DC system ,PV-/boost-INV system and PV-buck/boost-INV-AC system.

When these MPPTCC of 12 different PV systems are found ,a lot of advantages can be shown as follows: firstly, when PV system is designed ,it is easier to select the system configuration and calculate circuit element parameters, secondly, based on these MPPCC, the new MPPT control strategy can be designed easily because they clearly reveal the range of the varying control signal. Thirdly, according to these expressions shown by previous equations, the future MPPT operating effect of a PV system can be estimated by the historical data of solar irradiance, temperature and load in a certain area. Therefore these expressions can be used as theoretic guide during installation and commissioning periods for PV system

3.4. Perturb and Observe algorithm

The most commonly used MPPT algorithm is Perturb and observe method .it operates by introducing a small perturbation to the pv system, At each perturbation point the power of the module will change, if the power increases due to perturbation it continues in that direction. After we reach the peak power the power at the next instant decreases ,hence after that the perturbation decreases .the algorithm continues to operate in the same manner. the main advantage of this approach is the simplicity of technique. Furthermore previous knowledge of the PV panel characteristics is not required. In its simplest form this method generally exhibits good performance provided the solar irradiation does not vary too Quickly. At steady state the operating point oscillates around the MPP voltage and usually fluctuate lightly.

Maximum Power Point Tracking Constraint conditions

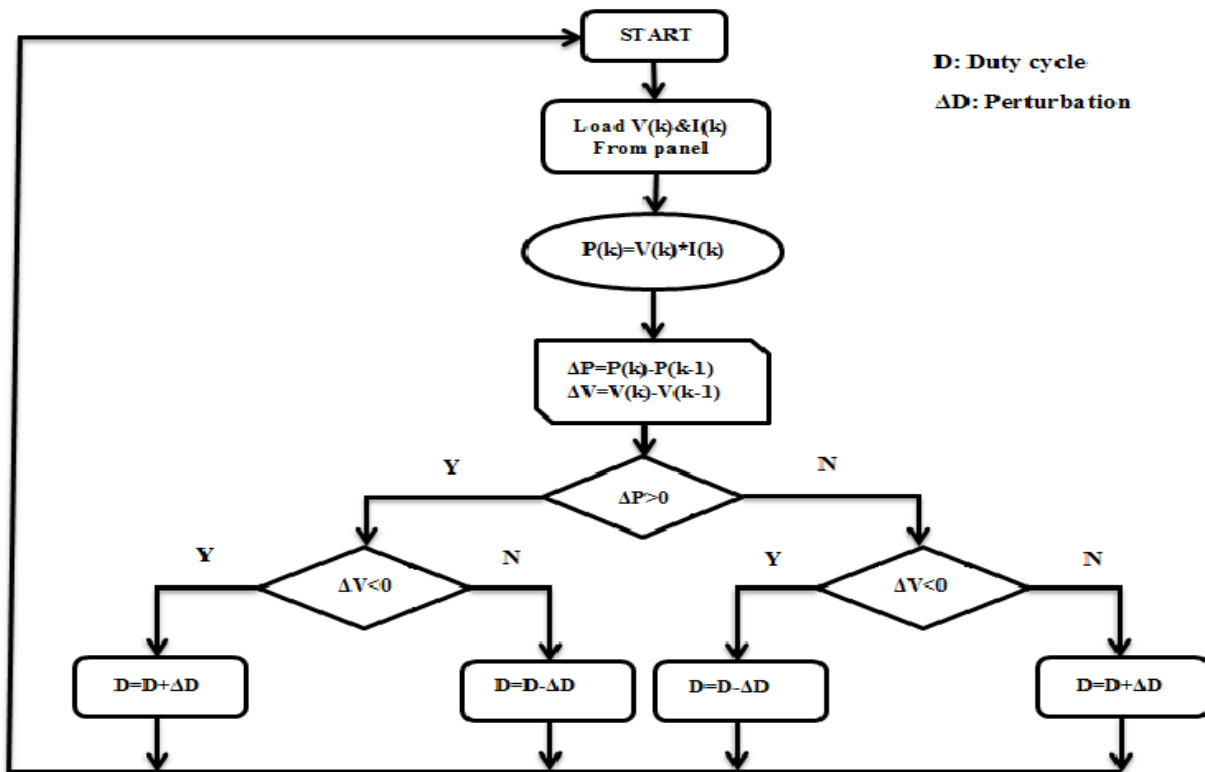


Fig.3.5.Flowchar of perturb and observe method [12]

3.5.A variable weather parameter MPPT method based on equation solution for photovoltaic system with DC bus

The control signals of the variable-weather-parameter (VWP) methods need to be calculated by the real time measured data of the irradiance and temperature (S&T) sensors, which leads to the high hardware cost of the sensors. To solve this problem, the PV system with a DC bus is selected as the research subject and a maximum power point tracking (MPPT) method is proposed, which is named the VWP MPPT method based on equation solution (ES-VWP method). The output maximum power point is directly calculated by solving the established equation. This equations set consists of two integrated mathematical equations which represent two different operating points of the PV system.

3.5.1.The principle of the ES-VWP method

3.5.1.1.Mathematical modeling of PV system with DC bus

Maximum Power Point Tracking Constraint conditions

In this section, the buck DC/DC converter or (buck circuit) is used as the MPPT circuit. For the PV cell , its mathematical model is shown by Eqs(3.1, 3.2 , 3.3) . It is usually called the four- parameter model [15].

Four the buck circuit, its model can be represented by Eq(3.84) and its input power (P_i) and output power (P_o) can be represented by Eq(3.85) and Eq(3.86), respectively.

$$V_o = DV \quad (3.84)$$

$$P_i = VI \quad (3.85)$$

$$P_o = V_o I_o \quad (3.86)$$

For the DC bus , its model can be represented by Eq(3.87)

$$V_o = V_{bus} \quad (3.87)$$

Assume that , under ideal condition , there is no power loss to the DC/DC converter , therefore :

$$P_o = P_i \quad (3.88)$$

According to Eqs (3.3) and (3.84)-(3.88), Eq.(3.89) is satisfied under ideal conditions.

$$P_o = \frac{V_{bus} I_{sc}}{D} [1 - C_1 (e^{\frac{V_{bus}}{C_2 V_{oc} D}} - 1)] \quad (3.89)$$

Eq.(3.90) is the integrated equation of the PV system with a DC bus under ideal conditions when the buck circuit is used .It can be used to establish the equation set which is the theoretical basis of proposing the new VWP method .

The control signal at the mpp can be calculated by Eq (3.90) for the PV system with a DC bus

$$D_{max} = \frac{V_{bus}}{C} \quad (3.90)$$

Where

$$C = C_2 V_{oc} [\text{lambertw} \left(e \times \frac{1+C_1}{C_1} \right) - 1] \quad (3.91)$$

Maximum Power Point Tracking Constraint conditions

Therefore , two different operating points A(V_1, I_1, D_1) and B(V_2, I_2, D_2) are first selected, and then Eq(3.92) and Eq(3.93) are given by submitting them into Eq(3.89) .

$$P_{o1} = P_{i1} = \frac{V_{bus}I_{sc}}{D_1} [1 - C_1(e^{\frac{V_{bus}}{C_2V_{ocD_1}}} - 1)] \quad (3.92)$$

$$P_{o2} = P_{i2} = \frac{V_{bus}I_{sc}}{D_2} [1 - C_1(e^{\frac{V_{bus}}{C_2V_{ocD_2}}} - 1)] \quad (3.93)$$

By substituting Eq(3.85) into Eq(3.92) and Eq(3.93) we get:

$$V_1I_1 = \frac{V_{bus}I_{sc}}{D_1} [1 - C_1(e^{\frac{V_{bus}}{C_2V_{ocD_1}}} - 1)] \quad (3.94)$$

$$V_2I_2 = \frac{V_{bus}I_{sc}}{D_2} [1 - C_1(e^{\frac{V_{bus}}{C_2V_{ocD_2}}} - 1)] \quad (3.95)$$

When two operating points A and B are different from each other as a result Eq(3.94) and Eq(3.95) are two independent equations. Therefore , an equation set can be established by combining them , then Eq (3.96) is presented

$$\begin{cases} V_1I_1 = \frac{V_{bus}I_{sc}}{D_1} [1 - C_1(e^{\frac{V_{bus}}{C_2V_{ocD_1}}} - 1)] \\ V_2I_2 = \frac{V_{bus}I_{sc}}{D_2} [1 - C_1(e^{\frac{V_{bus}}{C_2V_{ocD_2}}} - 1)] \end{cases} \quad (3.96)$$

To simplify Eq(3.96) ,Eq(3.84) and Eq (3.87) are substituting into Eq (3.96)

$$\begin{cases} I_1 = I_{sc}[1 - C_1(e^{\frac{V_{bus}}{C_2V_{ocD_1}}} - 1)] \\ I_2 = I_{sc}[1 - C_1(e^{\frac{V_{bus}}{C_2V_{ocD_2}}} - 1)] \end{cases} \quad (3.97)$$

The main principle of the ES-VWP method can be shown in the following figure

Maximum Power Point Tracking Constraint conditions

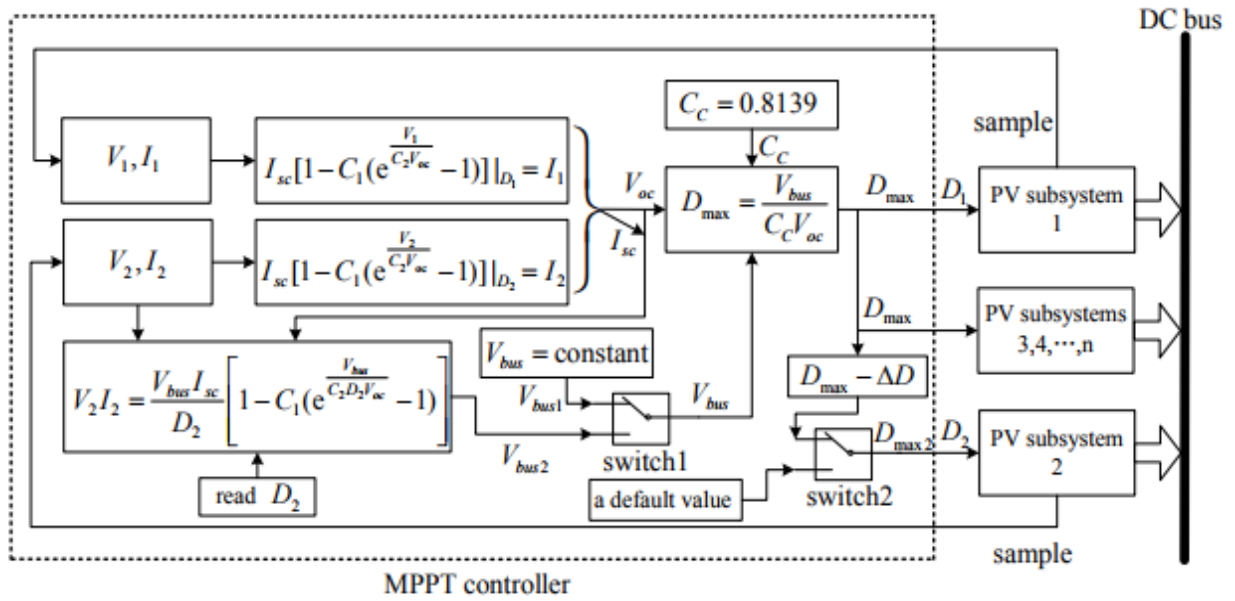


Fig3.6 The priciple of the ES-VWP.

Where : $D_{max2} = D_{max} - \Delta D$ (3.98)

The following flowchart is the design of the MPPT control process

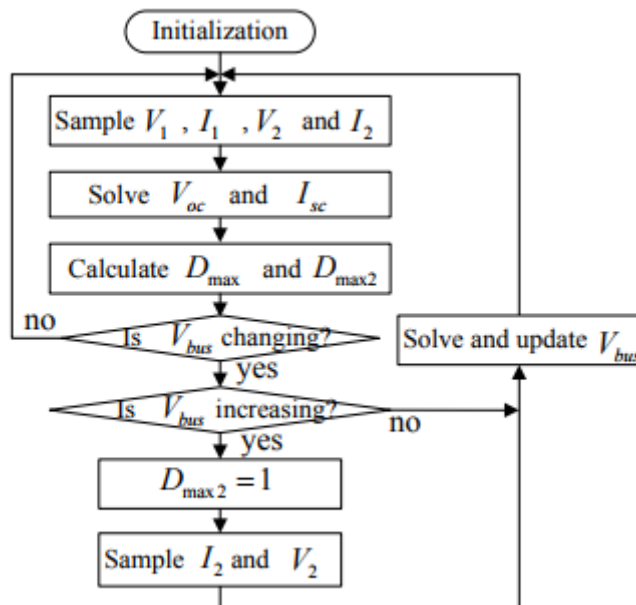


Fig.3.7 Flowchart of ES-VWP method.

Note that V_{bus} can be calculated from Eq (3.96).

Maximum Power Point Tracking Constraint conditions

3.6.Conclusion

This chapter investigate 12 different PV configurations , the reason to select these configurations which is illustrated as follows,these selected pv systems are more typical in real applications so findig their MPPTCC will insure the success of MPPT control. After we have established the MPPTCC of these 12 configurations ,other PV systems can be easily analyzed by analogy.In the other hand ,two equations of the PV system have been combined as an equation set to solve directly the real time V_{oc} and I_{sc} .In addition, an equation solution method that can estimate the real-time value of the DC bus voltage which is presented under unknown or varying bus voltage conditions .Based on them an ES-VWP method has been proposed.

CHAPTER 4
Simulation and discussion

Chapter 4 : Simulation and discussion

4.1.Introduction

In this chapter we are going to walk through the processes of simulation and result , involving 12 PV configurations MPPTCC and VWP using equation solution , these simulations will be carried out using MATLAB/SIMULINK tool.

4.2.Characteristics of C_R and C_c

To test the reasonableness of two assumed constant C_R and C_c , we use MATLAB/SIMULINK tool. The results are shown in figures below .Firstly C_R -S and C_c -S curves are given under 25°C and varying irradiance conditions ,secondly C_R -T and C_c -T curves are given under 1000W/m² and varying temperature conditions.

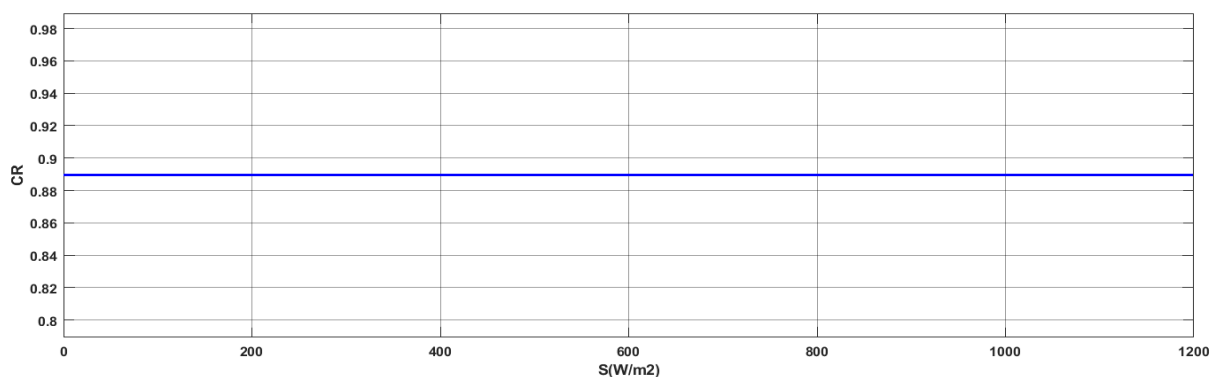


Fig.4.1. C_R -S curve

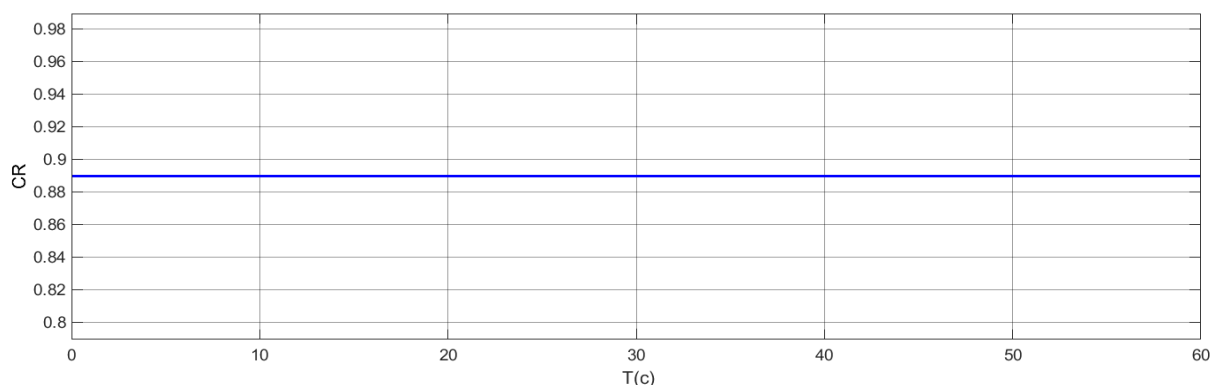


Fig.4.2 C_R -T curve

➤ Discussion:

Fig.4.1 Shows that C_R is constant when the irradiance vary ,Meanwhile, fig 4.2 shows that C_R always keeps constant under varying temperature. According to Fig.4.1 and Fig.4.2 C_R is about 0.889.

Chapter 4 : Simulation and discussion

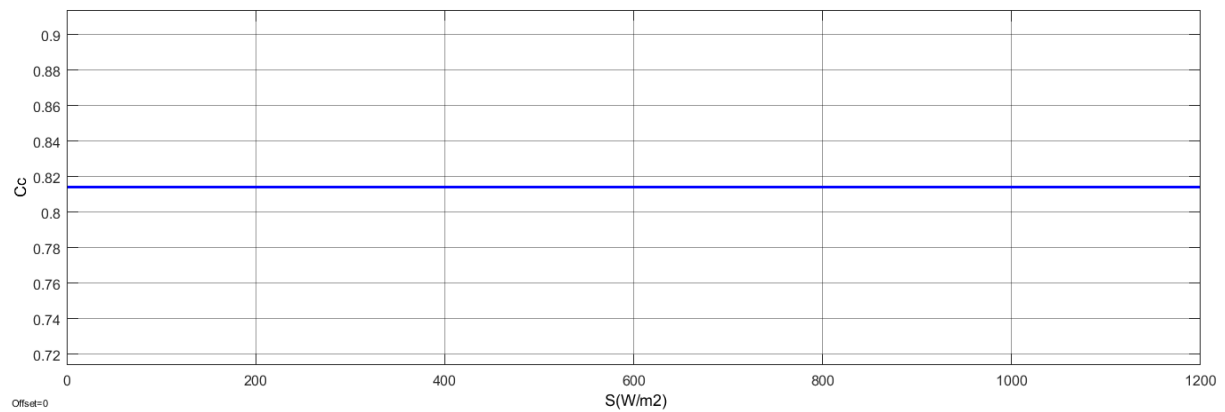


Fig.4.3 C_c -S curve

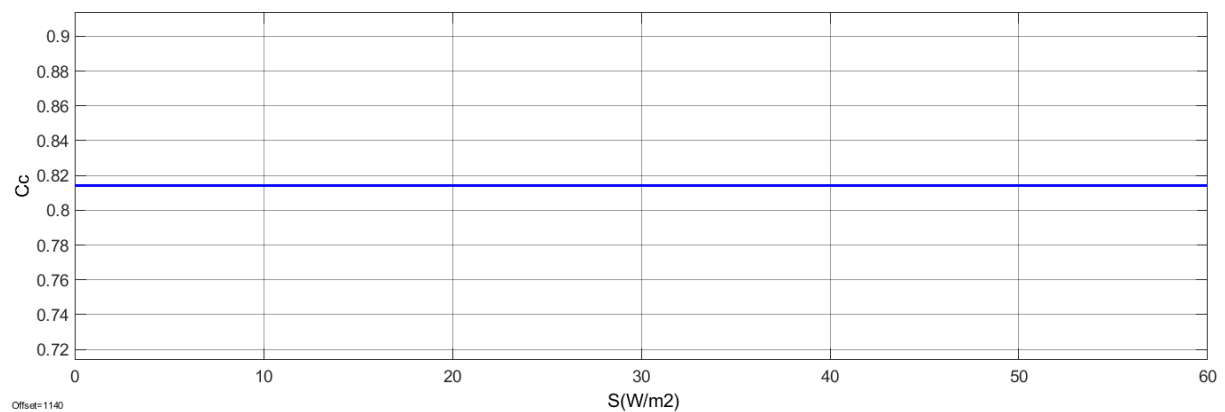


Fig.4.4 C_c -T curve

➤ Discussion:

Same thing for C_c it keeps constant under varying irradiance as we can see in Fig.4.4, also it keeps constant under varying temperature as drawn in Fig.4.3.

Note that the value of C_c is about 0.814.

4.3.Accuracy of the MPPTCC

In order to verify the accuracy of the MPPTCC which are proved from Eq(3.66) till Eq(3.83), we assume the values of D_L , D_U and M are 0.2, 0.8 and 0.80 respectively. The upper boundaries (UB) and the lower boundaries (LB) of the MPPTCC for all systems can be calculated and shown in Table 1.

Chapter 4 : Simulation and discussion

PV systems	Expressions of LB	Expressions of UB	Values of LB	Values of UB
PV-buck	$D_L^2 C_R V_{oc} / I_{sc}$	$C_R V_{oc} / I_{sc}$	0.085156	2.1289
PV-boost	$C_R V_{oc} / I_{sc}$	$C_R V_{oc} / [(1 - D_U)^2 I_{sc}]$	2.1289	53.223
PV-buck/boost	$C_R V_{oc} D_L^2 / [(1 - D_L)^2 I_{sc}]$	$C_R V_{oc} D_U^2 / [(1 - D_U)^2 I_{sc}]$	0.1331	34.062
PV-buck-DC	$C_C V_{oc} D_L$	$C_C V_{oc}$	3.5812	17.906
PV-boost-DC	$C_C V_{oc}$	$C_C V_{oc} / (1 - D_U)$	17.906	89.529
PV-buck/boost-DC	$C_C V_{oc} D_L / (1 - D_L)$	$C_C V_{oc} D_U / (1 - D_U)$	4.4764	71.6232
PV-buck-INV	$C_R M^2 V_{oc} D_L^2 / (2I_{sc})$	$C_R M^2 V_{oc} / (2I_{sc})$	0.02725	0.68125
PV-boost-INV	$C_R M^2 V_{oc} / (2I_{sc})$	$C_R M^2 V_{oc} / [2(1-D_U)^2 I_{sc}]$	0.68125	17.0312
PV-buck/boost-INV	$C_R M^2 V_{oc} D_L^2 / [2(1-D_L)^2 I_{sc}]$	$C_R M^2 V_{oc} D_U^2 / [2(1-D_U)^2 I_{sc}]$	0.04258	10.889
PV-buck-INV-AC	$D_L C_C V_{oc} M / \sqrt{2}$	$C_C V_{oc} M / \sqrt{2}$	2.0258	10.129
PV-boost-INV-AC	$C_C V_{oc} M / \sqrt{2}$	$C_C V_{oc} M / [\sqrt{2}(1-D_U)]$	10.129	50.6453
PV-buck/boost-INV-AC	$C_C M D_L V_{oc} / [\sqrt{2}(1-D_L)]$	$C_C M D_U V_{oc} / [\sqrt{2}(1-D_U)]$	2.5322	40.5162

Table 1 .The upper and the lower boundaries of the MPPTCC of all PV systems

To investigate the accuracy of the MPPTCC which is shown in Table1, some simulation experiments were carried out under $1000W/m^2, 25^\circ C$ conditions and the results are shown in the following figures .

Chapter 4 : Simulation and discussion

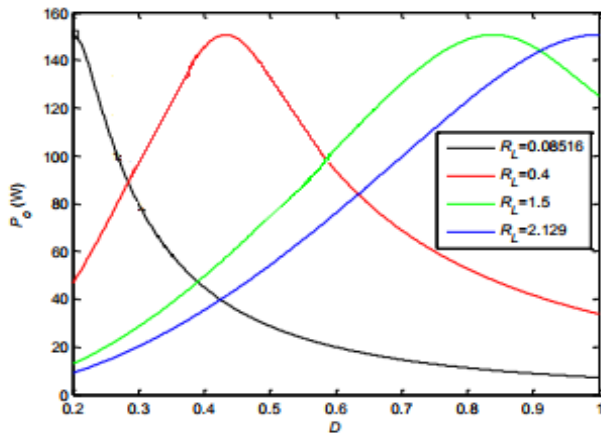


Fig.4.5 $P_o - D$ curve of PV-buck system

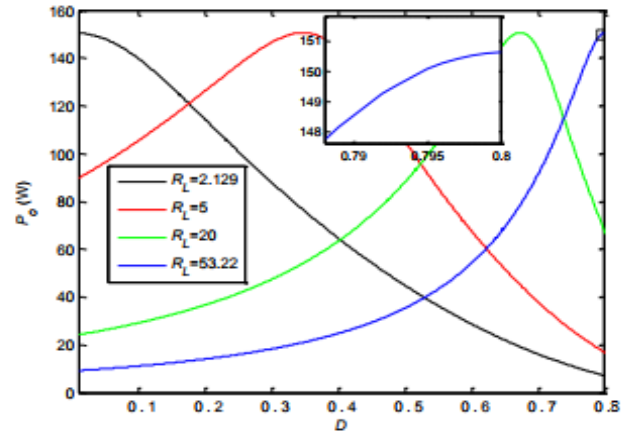


Fig.4.6 $P_o - D$ curve of PV-boost system

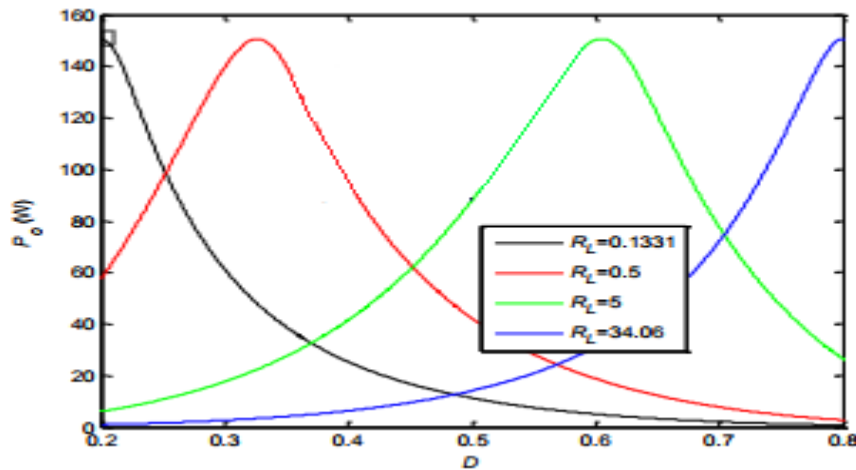


Fig.4.7. $P_o - D$ curve of PV-buck/boost system

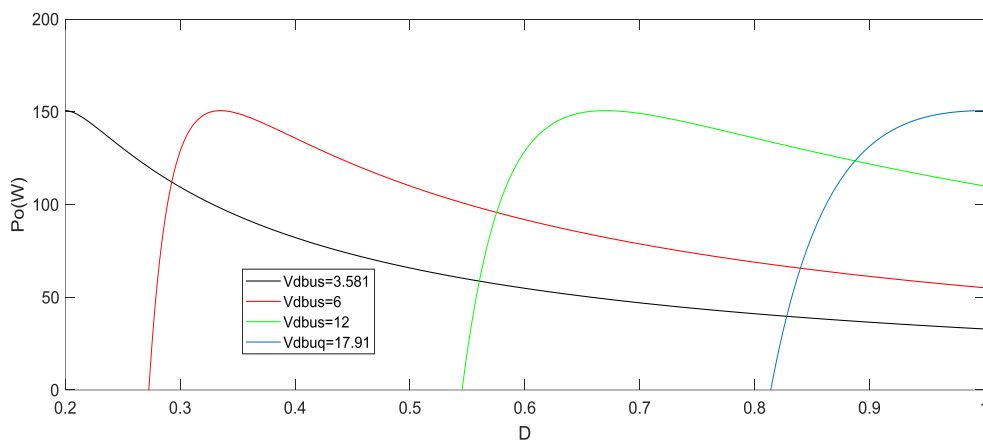


Fig4.8. $P_o - D$ curve of PV-buck-DC system

➤ Discussion:

Chapter 4 : Simulation and discussion

According to Figures 4.5,4.8, which represent PV-buck, PV-buck-DC systems respectively, their MPPs are achieved when $D=D_L$, in other word when the load resistance or bus voltages are equal to their corresponding LB. Figure 4.6 its MPPs reach when $D=0$, in other word when the load resistance equal to their corresponding UB., finally figure 4.7 its MPP is reached when $D=D_L$ such that the load resistances is equal to its corresponding LB and when $D=D_U$ such that the load resistance is equal to its corresponding UB.

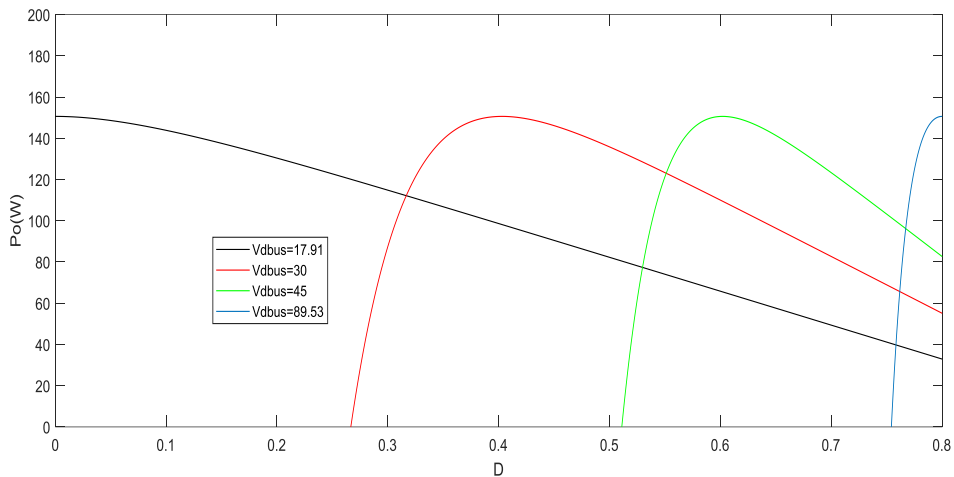


Fig4.9 $P_o - D$ curve of PV-boost-DC system

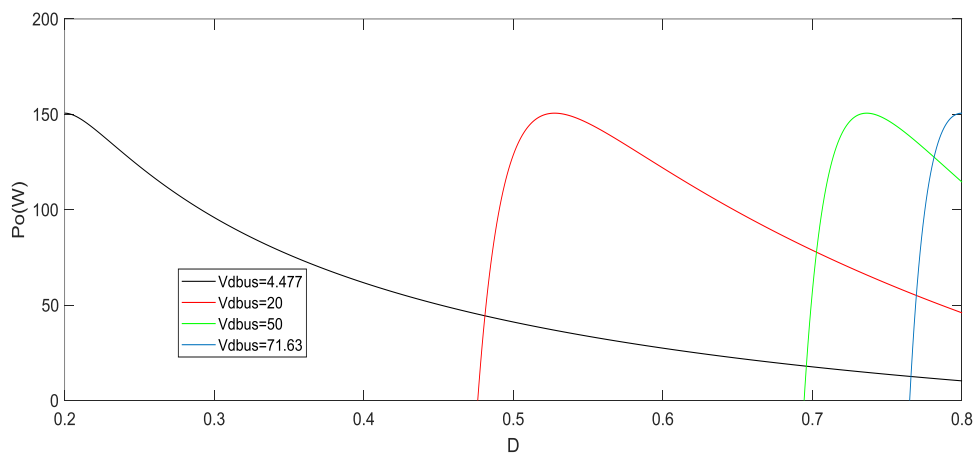


Fig4.10 $P_o - D$ curve of PV-buck/boost-DC system

Chapter 4 : Simulation and discussion

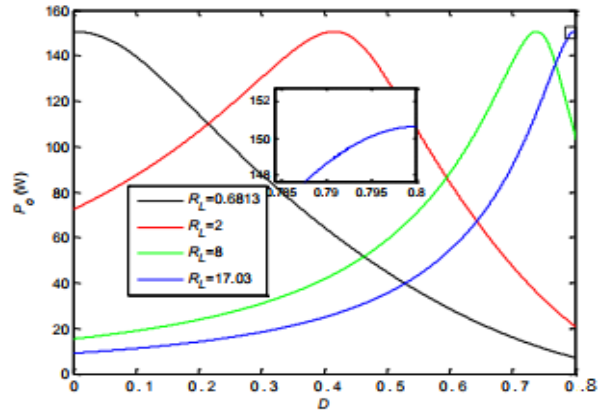
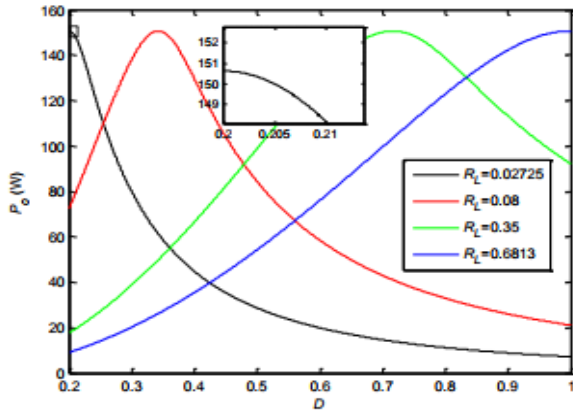


Fig.4.11 $P_o - D$ curve of PV-buck -INV system Fig.4.12 $P_o - D$ curve of PV_boost_INV

➤ Discussion:

Figure 4.9 and 4.12 , their MPPs reach when $D=0$, in other word when the load resistance or bus voltages equal to their corresponding UB. Figure 4.10 its MPP is reached when $D=D_L$ such that the load resistances is equal to their corresponding LB and when $D=D_U$ such that the load resistance is equal to its corresponding UB. Finally for the figure 4.11. MPP is achieved when $D=D_L$, in other word when the load resistance is equal to its corresponding LB.

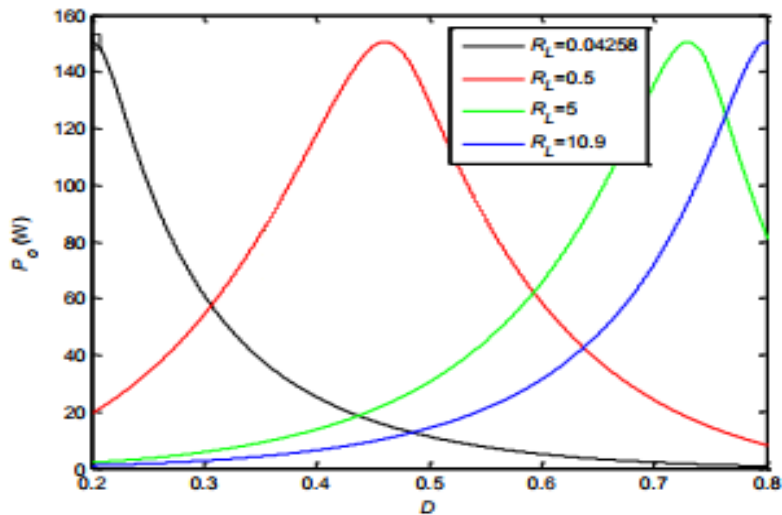


Fig.4.13 $P_o - D$ curve of PV-buck/boost-INV system

Chapter 4 : Simulation and discussion

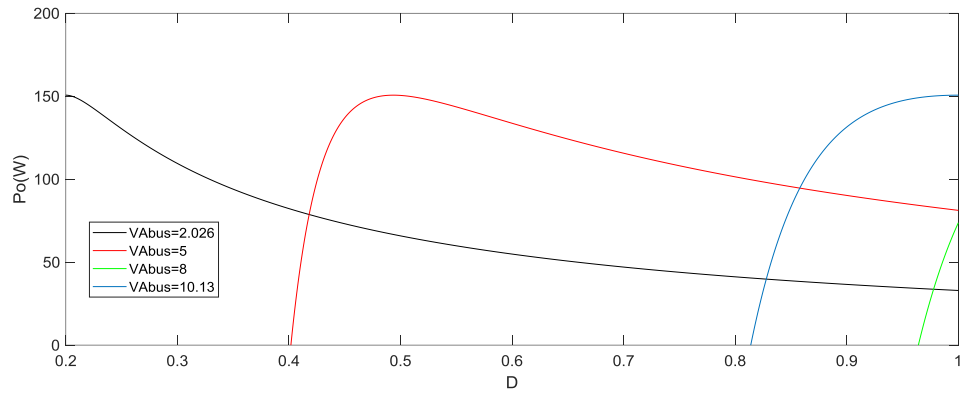


Fig4.14 $P_o - D$ curve of PV-buck-INV-AC system

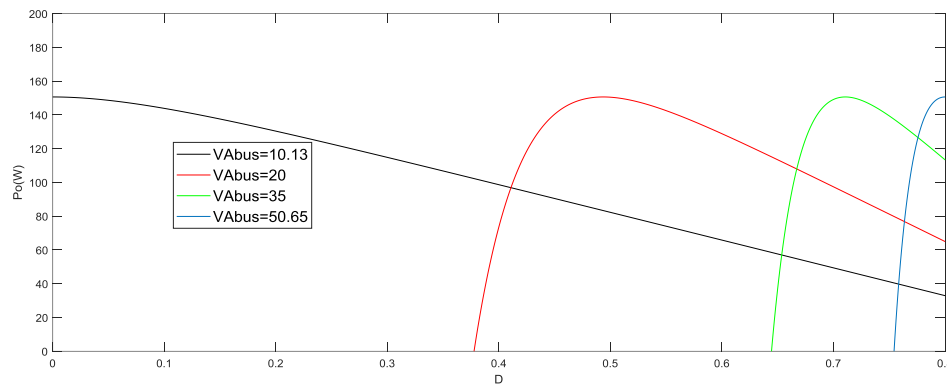


Fig4.15 $P_o - D$ curve of PV-boost-INV-AC system

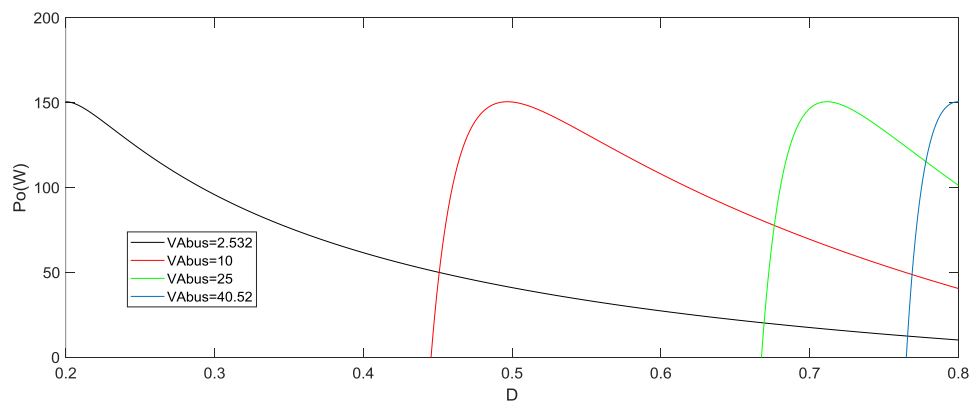


Fig4.16 $P_o - D$ curve of PV-buck/boost-INV-AC system

➤ Discussion:

According 4.14 , its MPP is achieved when $D=D_L$, in other word when the bus voltage is equal to its corresponding LB. Moreover, When the bus voltage is equal to UB the MPP will reach at $D=1$ condition. Figure 4.13,4.15, their MPPs reach when $D=0$, in other word when

Chapter 4 : Simulation and discussion

the load bus voltage or load resistance equal to their corresponding UB. Finally, Figure 4.16 which represents the graph of PV-buck/boost-INV-AC system, its MPP is reached when $D=D_L$ such that the load resistances or bus voltages is equal to its corresponding LB and when $D=D_U$ such that the bus voltage is equal to its corresponding UB.

4.4. Feasibility and availability of the proposed method

4.4.1. Analysis under varying S condition

To analyze the feasibility and availability of the ES-VWP method, some simulation will be carried out under 5 different S conditions, when T, V_{bus} , D_o and ΔD are set as 25°C, 15V, 0.8 and 0.001, respectively. The simulation results are shown in Table 2. I_{sc}^* and V_{oc}^* represent their solved values of I_{sc} and V_{oc} respectively and V_1^* , V_2^* , I_1^* and I_2^* represent the measured values of V_1 , V_2 , I_1 and I_2 respectively, D_{max}^* and D_{max2}^* represent the calculated values of D_{max} and D_{max2} respectively; P_{omax}^* and P_{omax2}^* represent the output powers of PV subsystem 1 and PV subsystem 2, respectively. Finally D_m represents the ideal value of D_{max} .

S (W/m ²)	V_1^* (V)	I_1^* (A)	V_2^* (V)	I_2^* (A)	V_{oc}^* (V)	I_{sc}^* (A)
300	17.8270	2.5225	17.8484	2.5195	21.9037	2.7571
400	17.5762	3.3636	17.5767	3.3596	21.5707	3.6761
600	17.2924	5.0477	17.3133	5.0417	21.2466	5.5149
700	17.3040	5.8885	17.3240	5.8816	21.2608	6.4336
950	17.7498	7.9893	17.7700	7.9800	21.8077	8.7300

D_{max}^*	D_{max2}^*	P_{omax}^* (W)	P_{omax2}^* (W)	D_m
0.8415	0.8405	44.9686	44.9690	0.8414
0.8545	0.8535	59.1193	59.0507	0.8544
0.8676	0.8666	87.2868	87.2884	0.8686
0.8658	0.8648	101.8946	101.8928	0.8658
0.8461	0.8451	141.8084	141.8046	0.8461

Table 2. Results under different irradiance condition

Chapter 4 : Simulation and discussion

➤ Discussion:

According to table 2, D_{max}^* is almost equal to its corresponding D_m under different S conditions, which means that the ES-VWP method is feasible, available and accurate, we notice that the error between P_{Omax}^* and P_{Omax2}^* is always less than 0.01W, which means that PV subsystem 2 is operating around the MPP.

4.4.2. Analysis under varying T conditions

To analyze the feasibility and availability of the ES-VWP method, some simulation will be carried out under 5 different T conditions when S , V_{bus} , D_o and ΔD are set as $1000W/m^2$, 15V, 0.8 and 0.001 respectively. Table 3 shows the results.

S (W/m ²)	V_1^* (V)	I_1^* (A)	V_2^* (V)	I_2^* (A)	V_{oc}^* (V)	I_{sc}^* (A)
0	19.1949	7.8854	19.295	7.8751	23.5839	8.6157
10	18.6792	8.0957	18.7025	8.0854	22.9503	8.8454
20	18.1636	8.3059	18.1856	8.2957	22.3167	9.0751
40	17.1322	8.7264	17.1518	8.7164	21.0495	9.5346
50	16.6166	8.9367	16.6350	8.9266	20.4159	9.8791

D_{max}^*	D_{max2}^*	P_{Omax}^* (W)	P_{Omax2}^* (W)	D_m
0.7815	0.7805	151.3564	151.9501	0.7814
0.8030	0.8020	151.2212	151.2172	0.8530
0.8258	0.8248	150.8650	150.8622	0.8258
0.8755	0.8745	149.5024	149.5019	0.8755
0.9028	0.9018	148.4975	148.4939	0.9028

Table 3. Results under different temperature conditions.

➤ Discussion:

According to table 3, D_{max}^* is almost equal to its corresponding D_m under different T conditions, which means that the ES-VWP method is feasible, available and accurate, also we notice that the error between P_{Omax}^* and P_{Omax2}^* is always less than 0.01W, which means that PV subsystem 2 is operating around the MPP.

Chapter 4 : Simulation and discussion

4.5 MPPT performance comparison

Some simulation are done to analyze the MPPT performance of the ES-VWP method. here we select D_0 and ΔD 0.8 and 0.001 respectively. V_{bus} is selected as 12 V, P&O method represents a conventional MPPT method. Therefore, it is used to compare with ES-VWP method. The results of P&O are the mean values of their oscillation.

4.5.1 Performance under varying S condition

Under varying S and 25°C conditions, two simulation are done, the result are shown together in Figs 4.17 and 4.18. The duty cycle curves are compared in Fig.4.17 while the output power curves are compared in Fig.4.18. The data corresponding to Fig.4.17 and 4.18 are shown in Table 4. Where $D_{max}^{\&}$ and $P_{omax}^{\&}$ represent the results of P & O method. D_{max}^* and P_{0max}^* represent D_{max} and P_{omax} of ES-VWP method.

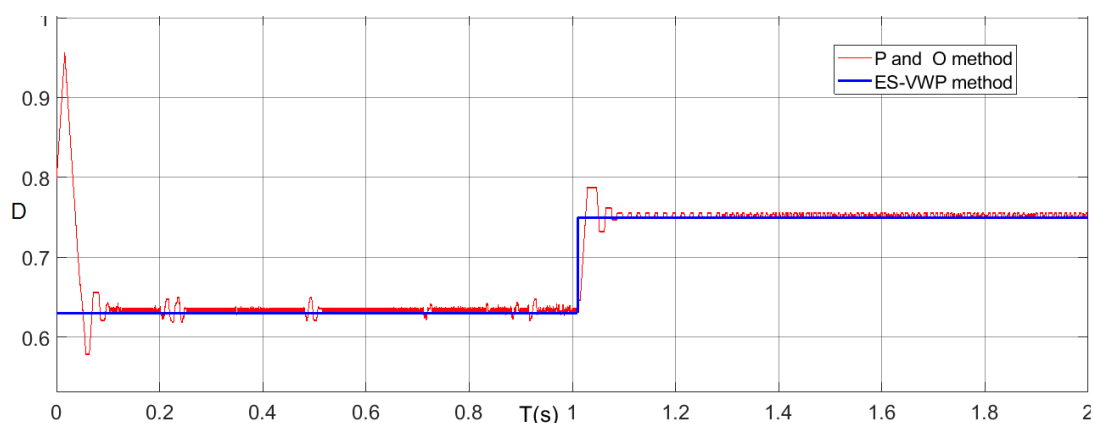


Fig 4.17 Simulation results of duty cycles

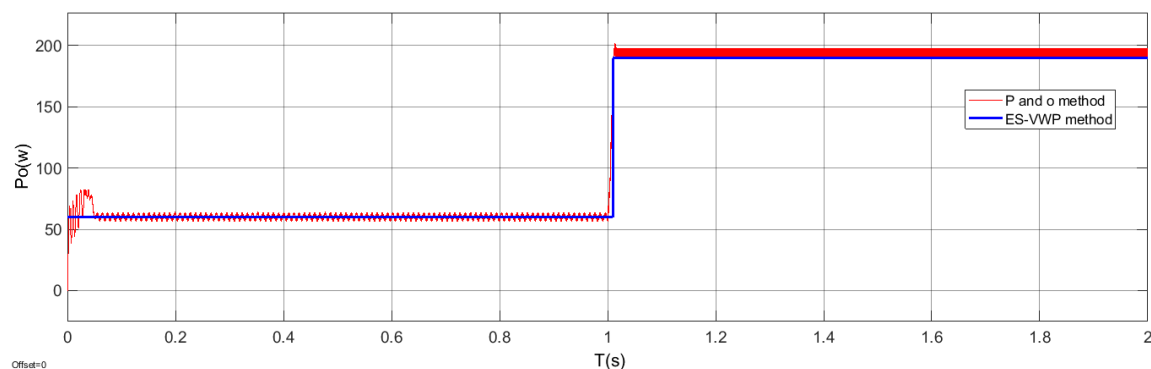


Fig. 4.18 Simulation results of output powers

Chapter 4 : Simulation and discussion

Time interval(s)	S (W/m ²)	Dm	Dm*	Dmax ^{&}	P _{omax} * (W)	P _{omax} ^{&} (W)
[0 1]	400	0.630	0.630	0.630	59.63	59.63
[1 2]	1200	0.752	0.752	0.751	189.41	189.41

Table 4. Result of Fig 4.18 and Fig 4.17

➤ Discussion:

Fig 4.17, Fig 4.18 and table 4 show that the MPPT speed of ES-VWP is better than P & O speed, since ES-VWP takes less transient time compared to P&O method. The steady-state oscillation exists in P & O method, therefore, the ES-VWP method has better steady state performance.

4.6.conclusion

After the analytical formulations were developed, the constraint conditions of the 12 widely used PV configurations were found, some simulations were carried out to verify the analytical results. The simulation results confirmed the integrated mathematical formulations and showed a good accuracy of MPP Constraint Condition. Moreover, ES-VWP was successfully designed and assessed on PV system with DC bus. The simulation results showed a better transient and steady state performance compared with the conventional P&O method.

General conclusion

General conclusion

In this project, an MPPTCC-based approach has been developed and examined on 12 widely used PV configurations. Its integrated mathematical formulations and constraints were elaborated and testified under ideal conditions through PV models' parameters. In this regard, several simulation experiments were carried out to assess the accuracy of these proposed MPPTCC approach. The inherent relationship between the model parameters and the Maximum Power Point as well the system components was exploited to design a more efficient MMPT control strategy. Moreover, an improved ES-VWP method has been successfully designed and assessed on a PV system with DC bus, and proved to be feasible and effective for MPPT applications. In effect, the simulation results have shown a better transient-state and steady-state performance compared with the conventional P&O method.

As a farther work on the subject, we intend to apply this approach for more practical models. Moreover, implementing the proposed approach on DSP or FPGA boards will be highly valuable to experimentally validate it for MPPT applications.

References

References:

- [1] David Thorpe, Solar Technology: The earth scan Expert Guide to using Solar Energy for Heating, Cooling and Electricity, Routledge, 1 edition, October 2011
- [2] Shaowu Li, a variable-weather-parameter MPPT control strategy based on MPPT constraint conditions. Energy conversion and Management, 2019,197:111873.
- [3] Shaowu Li, Aihong Ping, Yefeg Liu, Xiaohong Ma, Chao Li. A variable-weather-parameter MPPT method based on a defined characteristic resistance of photovoltaic cell.Solar energy, 2020,199:673-684.
- [4] View series: Hybrid Energy Systems,hybrid technologies for power generation, edited by:Massimiliano Lo Faro,Orazio barbera,Giosue Giacoppo,1st edition-October 30,2021.
- [5] Gow JA,Manning CD.Development of photovoltaic array model for use in power-electronics simulation studies.IEEE Proc Electro Power Appl 1999;146:193-200
- [6] Daniel F butay,Michael T.Miller.Maximum Peak Power Tracker : A Solar Application” Worcester Polytechnic Institute
- [7] website:<https://www.rcciit.org> (on 20/05/2022)
- [8] Akihiro Oi “Design and Simulation of Photovoltaic Water Pumping” thesis for the degree of Master of Science in Electrical Engineering, California Polytechnic State University, 2005.
- [9] Mirjana Milosevic: “On the Control of Distributed Generation in Power System” thesis for the degree of Doctor of Technical Sciences, Swiss Federal Institute of Technology Zurich, 2007
- [10] Home/Electronics Circuit’s/Power Electronics/DC-to-AC Converters (Inverters): Design,Working & Applications,Edited by; Pragya Chauhan,Last Updated : June 20,2021
- [11] R.Reshma Gopi, S. Sreejith.Converter topologies in photovoltaic applications.Renewable and Sustainable Energy Reviews,2018,94: 1-14

References

[12] Qiyu Li, Shengdin Zhao, Mengqi Wang, Zhongye Zou, et al. An improved perturbation and observation maximum power point tracking algorithm based on a PV module four-parameter model. *Applied Energy*, 2017, 195: 523-537.

[13] Shaowu Li. A maximum power point tracking method with variable weather parameters based on input resistance for photovoltaic system. *Energy Conversion and Management*, 2019, 197: 111873.

[14] [Researchgate.net/figure/perturb-and-Observe-Flow-chart_fig3_312292350](https://www.researchgate.net/figure/perturb-and-Observe-Flow-chart_fig3_312292350).

[15] Shaowu Li. A maximum power point tracking method with variable weather parameters based on input resistance for photovoltaic system. *Energy Conversion and Management*